Progress in Materials Science 142 (2024) 101244

Contents lists available at ScienceDirect

Progress in Materials Science

journal homepage: www.elsevier.com/locate/pmatsci

Multifunctional flexible and stretchable electrochromic energy storage devices

Libu Manjakkal [a,b,*], Luis Pereira [c,d], Eric Kumi Barimah [e], Paul Grey [c], Fabiane F. Franco [b], Zhengyu Lin [f], Gin Jose [e], Richard A. Hogg [b,g]

[a] School of Computing and Engineering & the Built Environment, Edinburgh Napier University, Merchiston Campus, EH10 5DT, UK
[b] James Watt School of Engineering (JWSE), University of Glasgow, Glasgow, G12 8LT, UK
[c] CENIMAT/i3N, Department of Materials Science, NOVA School of Science and Technology NOVA University Lisbon (FCT-NOVA) and CEMOP/UNINOVA Campus de Caparica, Caparica 2829-516, Portugal
[d] AlmaScience Colab, Madan Parque, 2829-516 Caparica, Portugal
[e] School of Chemical and Process Engineering, University of Leeds, Leeds LS2 9JT, UK
[f] Wolfson School of Mechanical, Electrical and Manufacturing Engineering, Loughborough University, UK
[g] School of Engineering and Applied Science, Aston University, B4 7ET Birmingham, UK

ARTICLE INFO

Keywords:
Energy storage
Flexible
Stretchable
Electrochromic
Supercapacitor
Battery

ABSTRACT

Electrochromic energy storage devices (EESDs) including electrochromic supercapacitors (ESC) and electrochromic batteries (ECB) have received significant recent attention in wearables, smart windows, and colour-changing sunglasses due to their multi-functionality, including colour variation under various charge densities. The performance of EESDs is mainly dependent on the properties of three major components (i) the current collector/substrate (cc/substrate) (ii) the electrolyte and (iii) electrochromic materials (ECM). Among various EESDs, advanced flexible or stretchable devices offer better functionality than conventional rigid glass-based devices and are easily integrated with any curved surface. However, in flexible or stretchable EESDs, delamination, dissociation and degradation critically affect the lifecycle and stable performance and are key issues to solve for widespread deployment of the technology. A detailed review of the materials and their performance as flexible EESDs is therefore propitious for the design and engineering of next-generation ECBs and ESCs. In this review, we considered the importance of various materials and their implementation in flexible and stretchable EESD fabrication along with their potential application in sustainable energy systems.

1. Introduction

For sustainable living and smart cities, the decarbonization of society is a central aim of energy research. Clean energy plays a key role in achieving global net-zero targets due to its direct decarbonization via electrification of buildings and transportation [1,2]. Intelligently using renewable energy sources like solar, wind, thermal, and mechanical is a promising option to achieve clean energy [3–6]. However, the proper and effective utilization of such energy generation requires an efficient long-term energy storage device with the capability of proper distribution of energy depending on end users and use cases [3,7–9]. The integration of energy generators

* Corresponding author at: School of Computing and Engineering & the Built Environment, Edinburgh Napier University, Merchiston Campus, EH10 5DT, UK.
E-mail address: L.Manjakkal@napier.ac.uk (L. Manjakkal).

https://doi.org/10.1016/j.pmatsci.2024.101244
Received 17 February 2023; Received in revised form 21 January 2024; Accepted 22 January 2024
Available online 27 January 2024

and storage will have a key role in the reduction of energy loss through proper energy distribution network design [10–14]. For this, recent developments in sustainable energy autonomous system technology have demonstrated remarkable performance in various applications including electric vehicles, smart buildings, robotics, unmanned aerial vehicles, wearable devices, and portable electric gadgets [15–22]. There are various self-powered systems designed using (i) integration of energy generator with storage and (ii) where combined energy generation and storage act as a self-powered device to achieve energy-autonomous systems for powering various electronic components [18,23–25]. In these systems, different types of energy storage such as batteries and supercapacitors (SCs) were used, depending on the requirement of high energy density and/or high power density.

Energy storage devices have been classified based on the type of electrodes involved in electrochemical reactions. During these electrochemical reactions in some of the materials, the electrode's colour variation occurs due to oxidation and reduction reactions. Such materials have been classified as electrochromic materials, and energy storage devices (batteries or SCs) developed using such materials are known as electrochromic energy storage devices (EESDs) [26–30]. As compared to traditional batteries and SCs, the EESD has been considered a promising candidate for the next generation of energy storage systems due to their multi-functionality such as (i) electrochromic properties (ii) energy storage capabilities and (iii) inherent energy storage level indication [28,31–33]. The major advantage of the EESD compared with traditional energy storages including SCs and batteries is its charging level determination via colour visualization, and the intensity of various colours (depending on the type of materials) protecting the device from overcharging [29,31,34]. The electrochromic nature saves energy in EESD. Due to these properties, the EESD could be used for intelligent applications as compared to traditional energy storage. Such EESDs could be potentially used as structural energy storage devices in eco-friendly sustainable energy autonomous system technologies [31,35–37] for a smart society as shown in Fig. 1. Studies on smart windows and wearable devices predict that the excellent optical, electrical, and electrochemical properties of EESDs and the sustainable materials used for their fabrication have many potential advantages compared with current energy storage devices, enabling the development of clean energy solutions.

Recent studies have shown that material formulation and electrode design are the critical steps to achieve high performance in EESDs [28,29,31,38,39]. Commonly reported devices use non-flexible glass-based electrodes [28,29,40–43]. However, due to electrochemical reactions, delamination of the electrodes, and electrolyte evaporation, result in the degradation of EESD performance over time [44,45]. Hence, due to these short life cycles, the development of EESDs on rigid glazed glass windows is not feasible for practical applications. Moreover, for wearable systems (e.g., lenses in sunglasses, sensors), flexible or stretchable devices are more suitable for curved surfaces (as shown in Fig. 1, the schematic of EESD). Moving towards the next generation of EESDs (replaceable smart window patches, wearables, or flexible electronics) requires the development of flexible or stretchable devices. This brings challenges including the fabrication of large-area electrodes, and the lengthening of the life cycle by solving the deterioration of the electrochemical properties due to delamination and electrolyte leakage during static/cyclic bending. To overcome such challenges, in-depth studies are required on flexible or stretchable EESDs. As compared to non-flexible EESDs, flexible or stretchable EESDs impose additional requirements of the material properties: (i) reliable electrochromic – electrochemical performance under various bending or stretching conditions and (ii) the EESD is normally exposed to ambient conditions so the device exhibits no solvent evaporation [37].

In this review, we provide a detailed analysis of flexible and stretchable EESDs for the development of smart energy systems. As compared with previous reviews in this area [28,29,44,46–49], we endeavour to provide a comprehensive review, which covers a wider range of materials including current collector/substrate (cc/substrate), electrolyte, cathodic/anodic electrode materials, separators, insulative/protective layers and packaging materials used for the fabrication of flexible and stretchable EESDs. A schematic

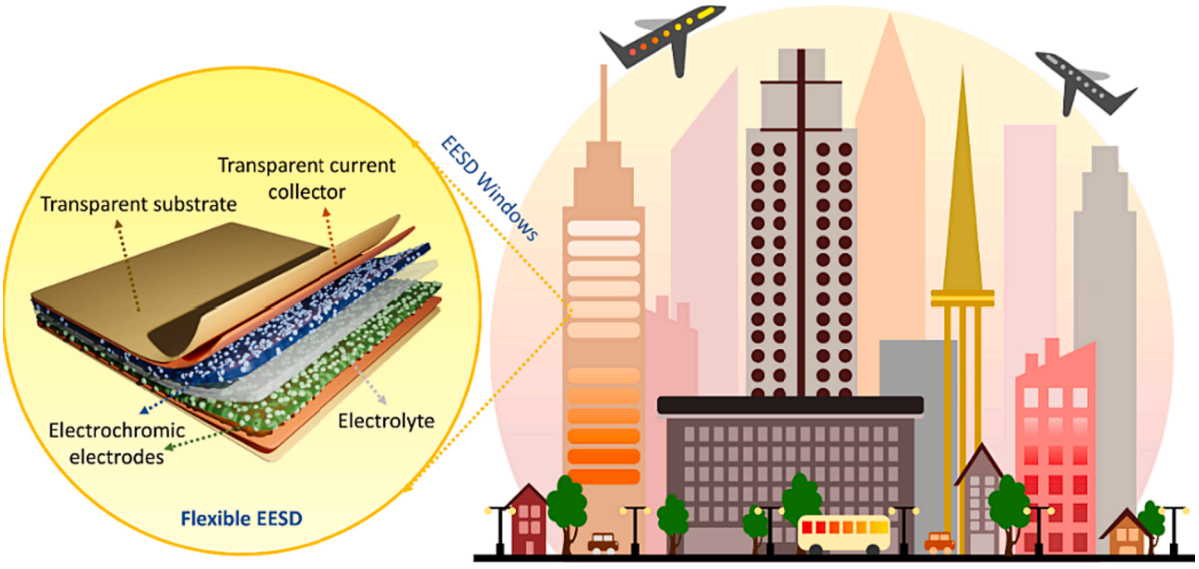

Fig. 1. The vision of EESDs for an advanced energy autonomous system for a sustainable society.

representation of the content of this review is summarized in Fig. 2. There are several reports on electrochromic windows developed using different materials, however, there is little or no discussion on their flexible energy storage properties [49,50]. Therefore, in this review, we discuss both the electrochromic and energy-storing performance of the devices. Following the introduction, in **section 2** we discuss the operating mechanism of EESDs. The classification of major EESD types and their methods of characterisation are described in **section 3**. There are various materials used for the fabrication of flexible or stretchable EESDs and a general overview of the prospective materials is summarised in **section 4**. One of the major requirements of smart windows is the control of spectral energy distribution for visual comfort by controlling the colouration efficiency (CE) and charge density of the EESD, which is explained in this review. We discuss the experimental methods for the performance evaluation of EESDs in terms of the charge density dependence on the colour of the window. The development of large-area flexible EESDs is very important for windows of smart buildings, aircraft and electric vehicles, and recent progress in this area is discussed in **Section 5**. The importance of flexible EESDs for the smart distribution of energy for smart windows, wearables, and energy-autonomous systems, including the utilisation of renewable energy sources with EESDs, is discussed in **Section 6**. **In Section 7**, we explore new approaches, which can improve the performances of EESDs and their potential future implementation.

2. Mechanism and development of EESD

The electrochemical reactions such as charge insertion/extraction or chemical oxidation/reduction processes produce a reversible change in colour for materials including WO_3 [55–57], V_2O_5 [58–60], TiO_2 [61–63], NiO [44,64,65], Polyaniline (PANI) [66–68] and PEDOT:PSS [59,69,70]. These reversible colour changes are clearly visible when those materials are deposited on the top of transparent cc/substrates. The schematic representation of an EESD with ions during charging and discharging is shown in Fig. 3**a**. The electrochemical reaction of these materials leads to charge storage and colour variation (transparent in discharged state and coloured in charged state) as shown in Fig. 3b [71] and Fig. 3c [72]. Similar to the mechanism of a rocking chair battery (lithium battery technology-mechanism), in EESDs when a voltage is applied between the cathodic and anodic electrochromic electrodes, ion transport occurs in one direction resulting in a colour change, and transporting ions in the reverse direction leads to decolourisation [28]. Due to the variation of applied bias, the colour of the EESD is modified as shown in Fig. 3d [71] depending on the oxidation and reduction reaction, as shown in Fig. 3b [71] and Fig. 3**c** [72]. The specific colour and amount of energy stored in an EESD depends on the type of

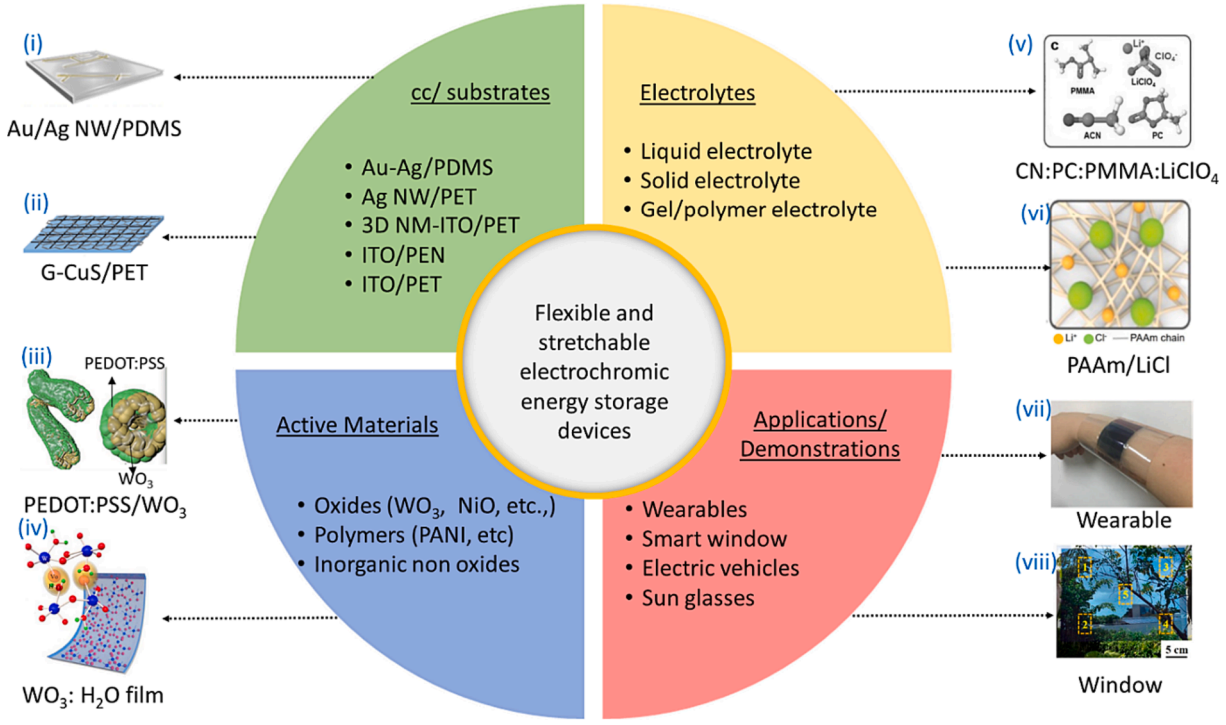

Fig. 2. Schematic illustration of the content of this review cc/substrates (i) Au/AgNW/PDMS "Reprinted (adapted) with permission from [37]. Copyright (2019) American Chemical Society". and (ii) G-CuS/PET [51], Reproduced from Ref. [51] with permission from the Royal Society of Chemistry. electrochromic materials (iii) PEDOT:PSS/WO_3 Reprinted (adapted) with permission from [37]. Copyright (2019) American Chemical Society and (iv) WO_3:H_2O film, Reprinted from Publication [52] Copyright (2021), with permission from Elsevier; electrolyte (v) CN:PC:PMMA: $LiClO_4$ Reprinted (adapted) with permission from [53] Copyright (2017) John Wiley and Sons (vi) PAAm/LiCl Reprinted (adapted) with permission from [37]. Copyright (2019) American Chemical Society; and applications (vii) wearable [54] (viii) smart window. Reprinted (adapted) with permission from [33] Copyright (2020) American Chemical Society.

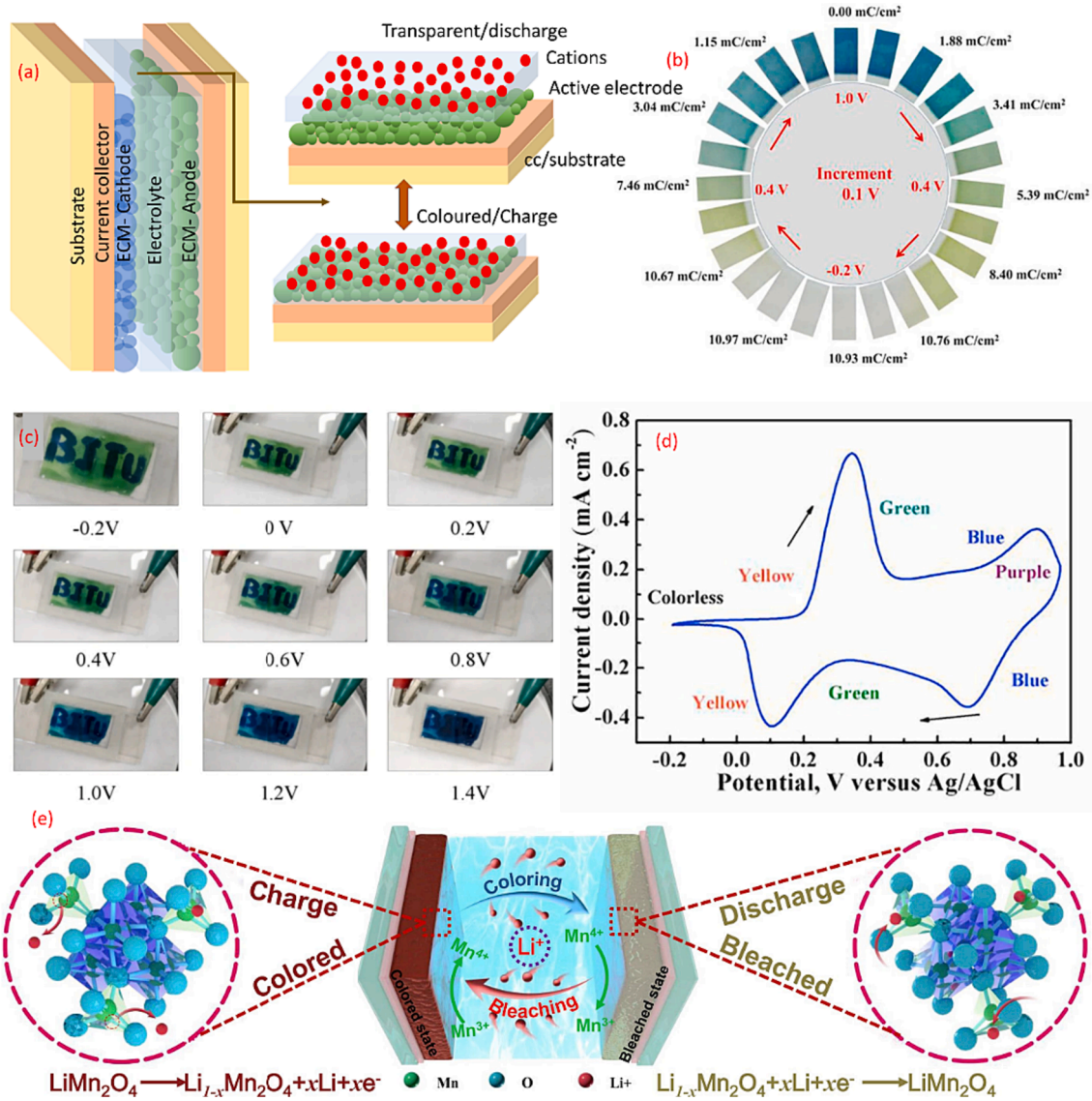

Fig. 3. (a) Schematic illustration of the EESD with cations during charging/discharging. (b) The colour evolution of the PANI film based EESD under different charge densities during the potentials sweeping. Reprinted from Publication [71] Copyright (2018), with permission from Elsevier. (c) Photo of ESC based on rGO–WNS and PANI electrodes at different voltage [72]. (d) Cyclic voltametric curve of PANI film electrode based EESD within the potential range of − 0.2 to 1.0 V. Reprinted from Publication [71] Copyright (2018), with permission from Elsevier (e) Electrochromic mechanism of LMO@LNO electrode during the electrochemical process based on Li-ions electrolytes [73]. Reprinted from Publication [73] Copyright (2018), with permission from Elsevier.

electrochromic material used. The charge density stored in the EESD determines the colour of the devices which allows the smart control of light and heat flow.

As mentioned above, the electrochemical reactions and colour change of these materials strongly depends on the type of the materials used for the fabrication. As an example, the colouring and bleaching mechanism during charging and discharging of an EESD based on $LiMn_2O_4$ electrodes coated with a $LiNbO_3$ thin layer (namely LMO@LNO) with a Li ion containing electrolyte ($LiClO_4$/ Propylene carbonate (PC) electrolyte) is shown in Fig. 3e [73]. During the electrochemical reaction, Li-ions in the electrolyte will undergo adsorption and diffusion at the electrode/electrolyte interface. The reversible redox reactions between Mn^{3+} and Mn^{4+} of the LMO@LNO electrode is accompanied by the insertion/extraction of Li-ions. Such insertion/extraction of ions leads to a change of the colour of the device that can be clearly measured by the variation in the transmittance spectra of the device [73].

3. Classification and characterisation of flexible EESD

The EESDs have mainly been classified as (i) electrochromic supercapacitor (ESC) [37,74–78] and (ii) electrochromic battery (ECB) [68,79–82]. These classifications are based on the type of materials, electrode configurations used in the fabrication, and their operation mechanism.

3.1. Flexible electrochromic supercapacitor

It may be observed that the majority of the reported flexible EESDs are ESC type. The operation of these ESCs is based on two key mechanisms depending on the type of material used for their fabrication (i) without any Faraday reaction in which charge storage is due to the surface-controlled ion adsorption and (ii) controlled Faraday reaction on the surface of the material or ion-intercalation [28,83]. The majority of electrodes used for the fabrication of these ESCs are carbon-based electrodes such as carbon nanotubes (CNT), graphene, reduced graphene oxide (rGO) and pesuodocapacitance materials including metal oxides (MO_x) and conducting polymers. A schematic representation of flexible ESC fabricated using CNT films and PANI hydrogel layers are shown in Fig. 4**a** [84]. Fig. 4b shows the corresponding image of the fabricated flexible ESC [84]. The electrochemical studies through cyclic voltammetry (CV) predict that the rectangular shape is due to non-Faradaic reactions which form electrical double layers (*edl*) and redox reaction peaks due to the pesuodocapacitance of PANI [84]. Theses electrodes show colour variation of (i) blue, green, light green, light yellow and yellow for the positive electrode and (ii) light yellow, yellow, light green, green and blue. The colour variation is shown for negative electrodes at different potential in Fig. 4c and its transmittance variation given in Fig. 4d [84]. Such flexible ESCs exhibit excellent promise for application in smart windows. An optical image of the porous CNT film is given in Fig. 4b. The detailed electrochemical and electrochromic properties of this device and other materials are discussed in the following section [84].

3.2. Flexible electrochromic battery

In ECBs, energy storage is based on diffusion-limited faraday reactions. The performance of the ESCs and ECBs show that the ECB stores more energy than the ESC and due to the slow diffusion-limited faraday reaction. This manifests itself in the ECB taking longer to charge/discharge as compared to an ESC [85]. Hence, it was noted that the development of flexible ECBs would significantly advance EESD technology in various applications. However, the fabrication of flexible ECBs is challenging due to the lack of proper electrochromic materials which have matching thermodynamic and kinetic properties [85]. The first reported flexible ECB was developed using electrodeposited Zn as the anode and electrodeposited polypyrrole (PPy) as the cathode and this rechargeable cell is denoted as Zn//PPy [85] (details discussed in materials section). Along with active electrode materials, the electrolyte and separator are critical in the ECB fabrication. For a flexible aluminium ion-based ECB fabrication, WO_3 coated PET/ITO was positive and Al sheet negative electrode where used along with $AlCl_3$ coated on an absorptive glass mat (AGM) as the electrolyte/separator. The AGM consists of superfine glass fibres that are highly porous and flexible as well as being chemically inert. The AGM absorbs the highly conductive $AlCl_3$ and exhibits high wettability [86]. Fig. 5**a** shows a schematic of the Al based flexible and rechargeable ECB. During electrochemical reaction Al^{3+} insertion occurs, and the cathodic reaction could be found in the peaks in Fig. 5b. The transport of Al^{3+} and

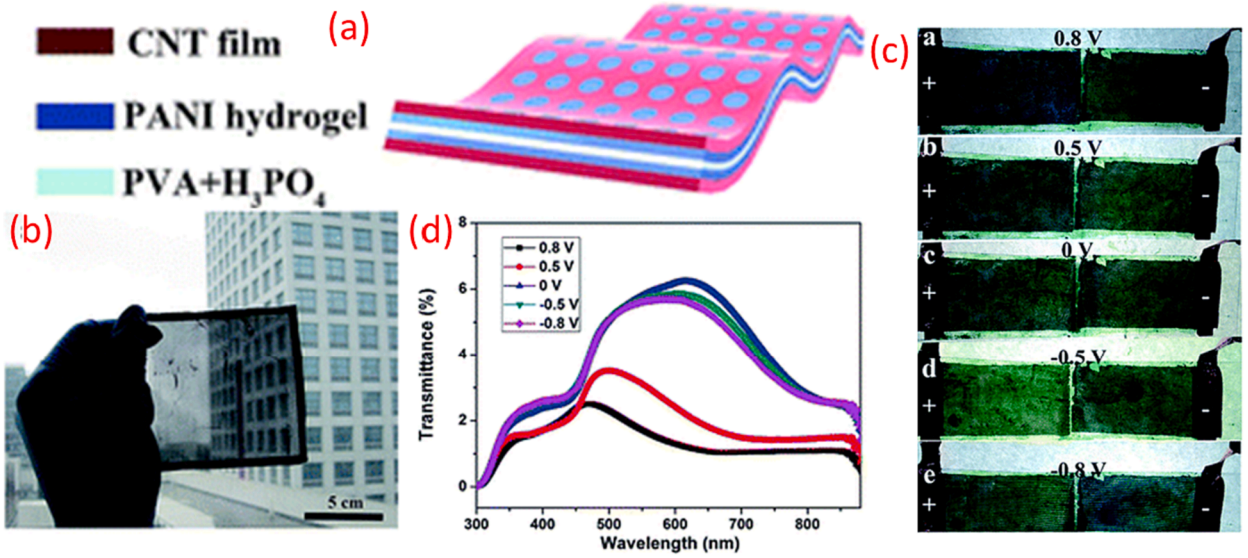

Fig. 4. Flexible ESC developed based on CNT and PANI hydrogel. (a) Schematic representation of the ESC (b) An image of the porous CNT film-based ESC. (c) Colour variation of the ESC in different potential (d) Transmittance variation of the EESD due to different voltage [84]. Reprinted from Publication[84] Copyright (2018), with permission from Royal Society of Chemistry.

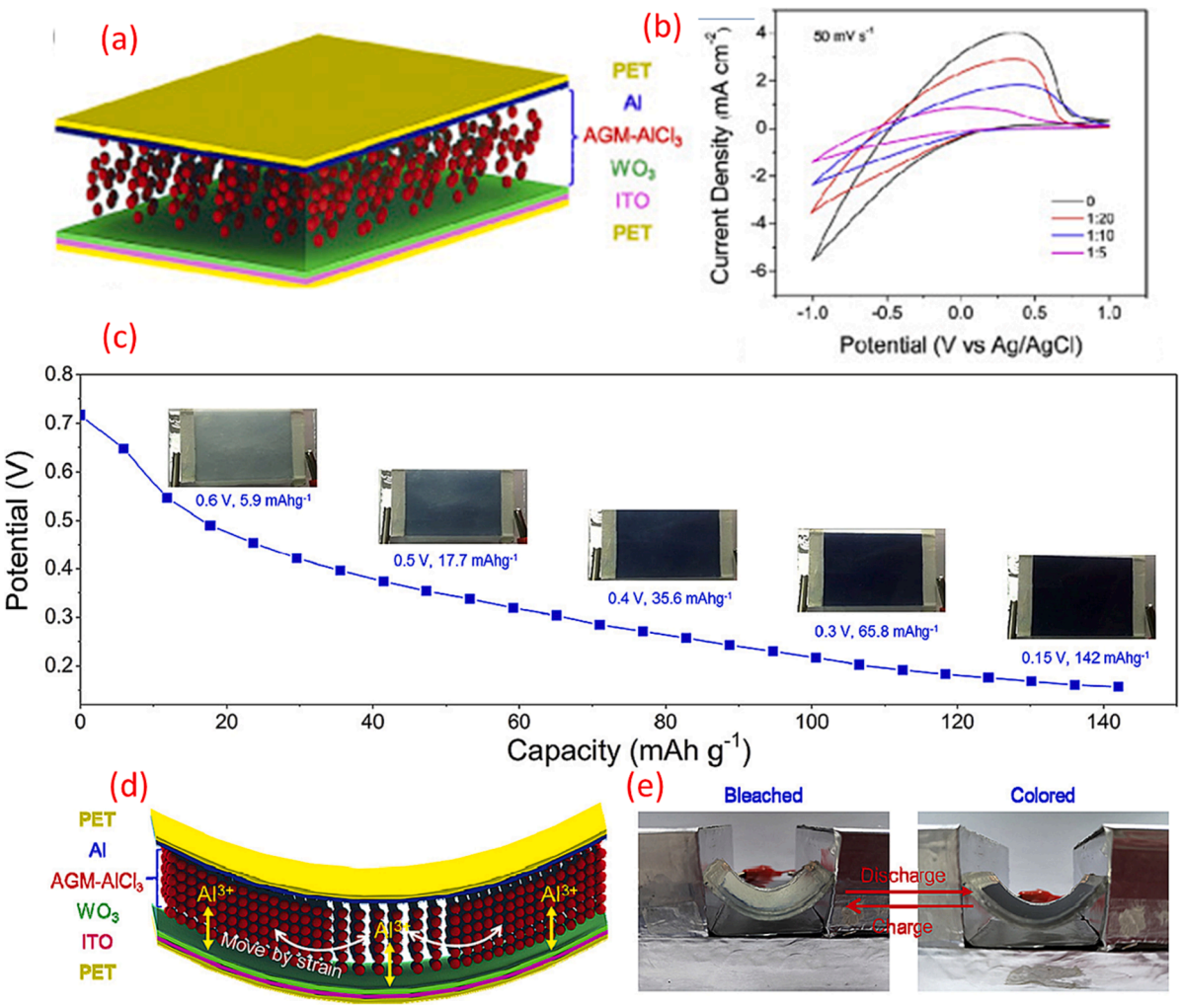

Fig. 5. Flexible ECB based on Al and WO_3 (a) Schematic representation of the device (b) CV curve for different O_2: Ar ratio in $AlCl_3$ electrolyte. (c) Variation of capacity with potential during discharge and inset shows images of the ECB at different capacity whilst discharging. (d) Schematic of the ions movement during bending and (e) The bleached and coloured state of ECB under bending [86]. (a-e) Reprinted from [86] Publication Copyright (2020), with permission from Elsevier.

electrons form aluminium tungsten bronzes (Al_xWO_3) which leads to the colouration process. The increase of Al^{3+} diffusion coefficient can be observed through the increasing redox peak of the CV curve at increasing scanning rates. The different capacity ranges during discharge are shown in Fig. 5c and the images in inset revealing its electrochromic performances at different potential. Additional work discussed that in this AGM based separator, the electrolyte was well distributed during bending. Even though the electrolytes are redistributed, remining Al^{3+} ions trapped in the pores of the AGM, schematic given in Fig. 5d are sufficient for electrochemical reactions and electrochromic performance. Associated images are given under bending conditions are given in Fig. 5d and 5e [86]. These studies of ECBs reveal that, the performance of the devices need to be improved and further detailed investigations of various materials are required.

3.3. *Characterisation of flexible EESD*

Based on their chemical, optical and physical properties there are three major characterisation steps required for the performance evaluation of flexible/stretchable EESDs. This includes electrochemical characterisation for specific capacity, energy storage and lifetime evaluation of the EESD. These values could be measured from CV, galvanostatic charging discharging (GCD) and electrochemical impedance spectroscopic analysis (EIS). Electrochromic characterisation is required for analysis of the transmittance modulation, colouring time (T_c) and bleaching time (T_b) prediction, visible colour variation and colouration efficiency (CE). The CE value is measured from the optical density (OD) and the inserted charge in unit area (Q) [87].

$$CE = \frac{\Delta OD}{Q} = \frac{\log\left(\frac{T_b}{T_c}\right)}{Q}$$

The observed electrochemical performances and CE values for EESDs of different materials are summarised in Table 1. For example, rGO/WO_3 based EESDs demonstrated a specific capacitance of 406F. g^{-1}, energy density 40–6 to 47.8 W.h. Kg^{-1}, power density 6.8—16.9 kW. Kg^{-1} and CE value of 64.8 cm^2. C^{-1}. Table 1 summarises that depending on type of material the performance of EESDs will vary. In addition to this for flexible or stretchable EESDs, dynamic bending and cyclic bending, tensile strength analysis, delamination issues prediction, atmospheric influences (humidity and temperature) and finally the washability in the case of wearables need to be monitored. A thorough evaluation of these aspects will help to choose the proper material and method of fabrication for future smart EESDs.

4. Materials for the fabrication of flexible EESD

In this section, we discuss relevant materials including current collector, substrate, electrolyte and electrochromic cathodic and anodic electrodes used for the fabrication of flexible and stretchable EESDs. We compare the properties and performance of different materials used in ESCs and ECBs.

Table 1
Electrochromic and electrochemical performances of various flexible and stretchable EESD.

Material	Electrolyte	Capacity	Energy density	Power density	Properties	Electrochromic functions	ref
AgNW/WO_3	1 M H_2SO_4	13.6 mF.cm^{-2} (138.2F.g^{-1}) at 10 mV.s^{-1}			− 72.6 % capacity retention after 5000 charge/discharge cycles	- transmittance of 55.9 % T_c − 1.7 s and T_b – 1.0 s CE − 80.2 cm^2.C^{-1}	[75]
NiCo-BH@ 3D NM	2 M KOH	68.61 μA. h. cm^{-2} at 1 mA. cm^{-2}	75.58 μA. h. cm^{-2}	51.46 μW. h. cm^{-2}	− 83.7 % capacity retention after 15 000 cycles –No significant variation in 0° to 180° of bending	fully charged situation (1.434 V) the devices shows blackish green and after fully discharge brown colour	[96]
PEDOT: PSS and Ag nanowire		0.58 mF. cm^{-2} at 0.1 V. s^{-1}	–	–	–	Transmittance- 35 % at a wavelength of 650 nm at a voltage of −1.8 V -T_c- 1.6 s and T_b − 2.0 s	[104]
rGO-WNS (cathode) – PANI (anode)	1 M H_2SO_4	13.98 mF. cm^{-2} at 0.2 mA. cm^{-2}				Tc- 18 s and T_b- 13 s -CE 76.37 $cm^{-2}C^{-1}$	[72]
WO_3	1 M H_2SO_4	13.6 mF.cm^{-2}, (138.2F. g^{-1}) at 10 mV. s^{-1}			− 72.6 % capacitive retention after 5000 charge/discharge cycles	- T_c − 1.7 s, T_b- 1.0 s - CE 80.2 cm^2. C^{-1}	[75]
PANI	0.5 M H_2SO_4	17.3 mF. cm^{-2} at 0.025 mA. cm^{-2}				-optical modulation 40.1 %	[51]
PANI	0.5 mol/L H_2SO_4	473.3F. g^{-1} at 0.03 V. s^{-1}				CE − 80.9 cm^2. C^{-1} and transmittance 49 % at the wavelength 630 nm	[71]
polyFe/ITO/ PET film			18.24 mA. h. g^{-1}			Ce- 717.2 cm^2. C^{-1} T_b- 1.7 S T_c − 1.4 S	[33]
polyFe/ITO/ PET film and TiO_2/ ITO/PET	$LiClO_4$/ PMMA					CE- 728.7 cm^2. C^{-1} T_b- 0.8 s T_c – 0.6 s	[33]
Zn//PPy	PVA gel based on KCl and Zn $(CH_3COO)_2$ in		123 mA. h. g^{-1} at 1.9 A. g^{-1}				[85]
rGO/WO3 on the top of AgNW/ CNF		406.0 F. g^{-1}	40.6 –47.8 W. h. kg^{-1}	6.8–16.9 kW. kg^{-1}	94.1 % capacitance retention after 10,000 cycle of charging - less influence during mechanical bending	CE- 64.8 cm^2. C^{-1} 75 % CE retention after 10,000 cycle charging discharging	[53]
PANI on the top of PEDOT: PSS/PET	H_2SO_4 -PVA	0.017F. cm^{-2} (400F. cm^{-3})			30 % transmittance for the ESC		[123]

4.1. Current collector/ substrate

In an EESD, the major requirements for the current collector is low sheet resistance, high transmittance, stable mechanical and electrochemical performance, and high Figure of Merit (FoM) value [54]. Mechanical flexibility or stretchability are additional features required for the substrate and current collector. In general, transparent conductive oxide (TCO) films such as indium tin oxide (ITO) or fluorine-doped tin oxide (FTO) coated on the top of glass are used for the cc/substrate [32,88]. To overcome the non –flexibility of ITO and FTO coated on glass substrates, recently there has been considerable recent interest in ITO coated polymer/ plastic substrates. For example, ITO coated polyethylene terephthalate (PET) is the most commonly used cc/substrate for flexible EESD fabrication. Here, the PET offers excellent transparency (>85 %), low weight, temperature stability (<100 °C), high flexibility and excellent barrier properties [89,90]. The PET substrate may be converted into a conductive material via coating a thin film of ITO which shows very low resistance coefficient (0.0001 Ω/cm). High light transmission coefficients (more than 90 %) [91] are due to the wide band gap and low free carrier density in a thin ITO layer [92]. Even though ITO shows excellent electrochromic performance, poor stability of this material when coated on polymer substrates, high material defect structure, and reduced activation efficiency of the tin dopant on the top of polymer/plastic substrates bring difficulty in obtaining high quality flexible ITO films [90]. Moreover, the delamination of ITO during bending and high material cost (especially indium) forces the search for an alternative material [91]. In addition to this, extreme anodic or cathodic polarization whilst working outside its operating potential window degrades the ITO causing the loss of conductivity and transparency [93].

Recent studies have addressed these issue through the fabrication of flexible current collectors including carbon nanotubes (CNT), graphene, metallic (Ag or Au) nanowires (NW) and conductive polymers on flexible substrates including PET, poly vinyl chloride (PVC) and polydimethylsiloxane (PDMS) [54]. Among the various current collector materials, Ag NW based current collectors have excellent properties for electrochromic devices due to their ability to maintain high conductivity over many bending cycles. One of the advantages of using Ag NW networks for the current collector of an EESD is its decreasing transmittance in the near infrared (NIR) region. For smart window applications, lowering the NIR transmittance will allow a decrease in the indoor temperature (especially during high solar loads), reducing the energy consumption for climate controlled buildings [53]. However, the oxidation of Ag results in reduced conductivity and to overcome this, recently Au/Ag core – shell NWs with high oxidation resistance and Ag NW networks were embedded into PDMSs [37]. These Au/Ag core – shell and Ag nanowires are not fully encapsulated by PDMS, i.e., partially embedded in PDMSs and partially exposed on the surface. This helps to enhance the adhesion and maintain the electrical conductivity during stretching [37]. The metal NWs exhibit excellent transparency, conductivity, and flexibility.

As mentioned above, oxidation and corrosion during electrochemical reaction is a major disadvantage of metal NWs for implementing EESD fabrication. To overcome this, CNTs which offer excellent stability during electrochemical reaction, good conductivity and flexibility is proposed as a promising alternative [90]. Its electrical conductivity and flexibility can be further enhanced by incorporating CNTs with conductive polymer networks [90]. Based on their performance CNT/polymer/substrate structures promise to be one of the future cc/substrates for flexible EESD fabrication [90]. In flexible EESDs, another major issue is deterioration of the

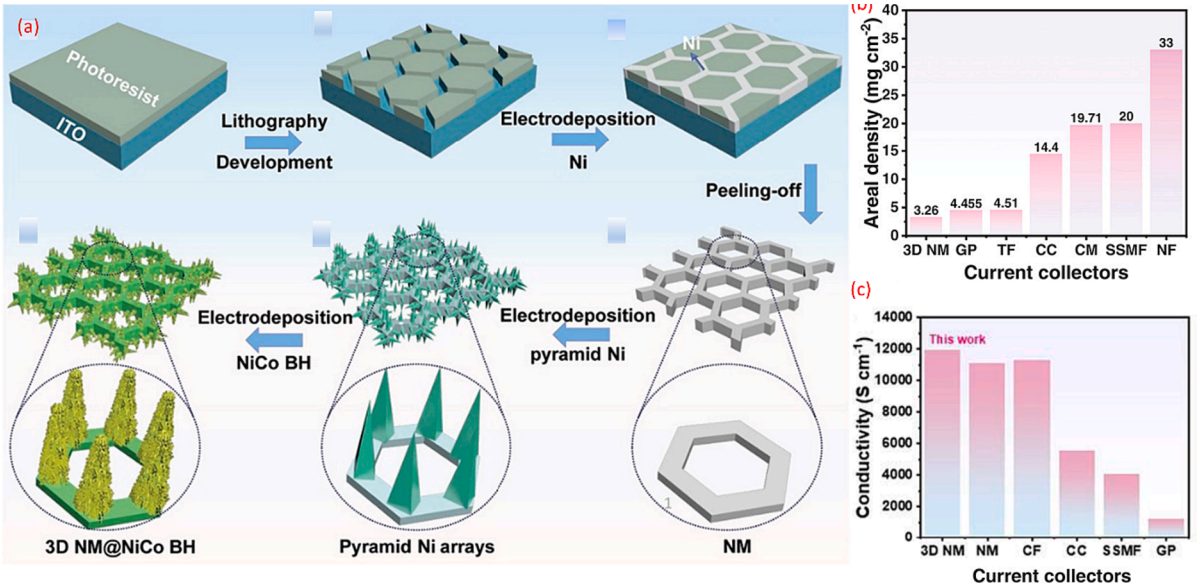

Fig. 6. (a) Schematic illustration of fabrication process of the 3D NM current collector and 3DNM@NiCo BH electrode based EESD via photolithography and electrodeposition [96]. (b) and (c) Comparisons of areal density and conductivity of various current collectors. 3D NM (thickness: 4.79 μm), graphite paper (GP, thickness: 25 μm), titanium foil (TF, thickness: 10 μm), copper mesh (CM, thickness: 62 μm), carbon cloth (CC, thickness: 300 μm), stainless steel mesh foil (SSMF, thickness: 30 μm), and nickel foam (NF, thickness: 100 μm) [96]. Reprinted (adapted) with permission from [96] Copyright (2021) John Wiley and Sons.

electrochemical properties due to delamination during multiple bending cycles. Wrapping with layers such as carbon, Al_2O_3 and Fe_2O_3 has been used in the current collectors (Ag NW coated PET, PDMS, and PU) to solve the delamination issue [94,95]. Even though these layers prevent delamination, they are used as a buffer layer without any contribution to the electrochemical properties. Additionally, they are brittle in nature [37].

For the design of a flexible current collector, 3D architecture [96] offers excellent rigidity, large thickness, and loading surface area. This architecture may provide ultra-lightweight, highly conductive current collectors and the active material is easy to integrate with this electrode. Recently an ultra-lightweight 3D Ni micromesh (3D NM) on ITO sheet was prepared by photolithography and electrochemical deposition technologies as shown in Fig. 6**a** along with preparation of the Ni–Co bimetallic hydroxide (3D NM@NiCo BH) as an active electrode [96]. The 3D structure of the current collector allows larger areas of active material, with highly conductive and ultrathin features allowing lightweight, flexible and high gravimetric energy density. The areal density of the 3D NM (3.26 mg. cm^{-2}) is superior to the values of the current collectors commonly used in flexible energy storage devices as shown in the comparison Fig. 6b [96]. This improved areal density is achieved by combining fabrication methods including photolithography and electrodeposition technology. The high electrical conductivity of the 3D NM [96] compared with other current collectors are presented in Fig. 6c. In addition to the electrical conductivity, tensile strength (for 3D NM 76 MPa and for normal NM 44 MPa), and stable resistance value before and after 4000 bending cycles shows the superior performances of the 3D NM for EESD along with its dark gray colour [96]. In addition to flexibility, stretchability is another important factor in wearable devices. The proposed 3D structure could be potentially used for stretchable applications. There are several reports of stretchable conductive electrodes, sensors, and energy storage devices based on stretchable polymers of polyurethane (PU), PDMS *etc.* [37]. However, simultaneously obtaining both high optical transparency and high electrical conductivity in a single stretchable electrode is challenging. Transparent conductive materials transferred to stretchable substrate demonstrate low conductivity, and during stretching delamination may also occur. However, AgNW embeded in polymer matrix (crosslinked poly(acrylate) matrix) shows excellent electrical ($50\Omega sq^{-1}$) and optical (92 % transparency) properties [97]. The first stretchable elastomeric electrochromic device was reported based on the facile and direct transfer method of AgNW into the PDMS substrate [98]. The AgNWs were transferred from a hydrophobic teflon plate, and this transferred conductive network shows excellent FoM values due to the high transmittance of 83 % and sheet resistance of 20 Ω sq^{-1}. In future stretchable or flexible EESD fabrication optimisation of the amount of AgNW deposition is very important because larger thicknesses of AgNW may prevent the transmission of light [98].

The polymers have many advantages including high conductivity, multi-colouration, ease of synthesis, low temperature coating, high CE values, low weight, and high flexibility. Conjugated polymers may provide both *edl* formation and pseudo-capacitance to enhance the capacity [90]. To overcome the electrochemical stability issues of the polymer, coating with CNT is a promising method. Such polymer/CNT composites exhibit excellent electron-transport and stability due to the strong π-π interactions or extended conjugation lengths of the polymers through covalent grafting [90]. Recently, PANI-CNT coated on PET has shown excellent electrical (364 Ω/□), optical (visible range 94 % and after −0.4 V applied the transmittance enhanced to 97 %) and mechanical (100 %–120 %

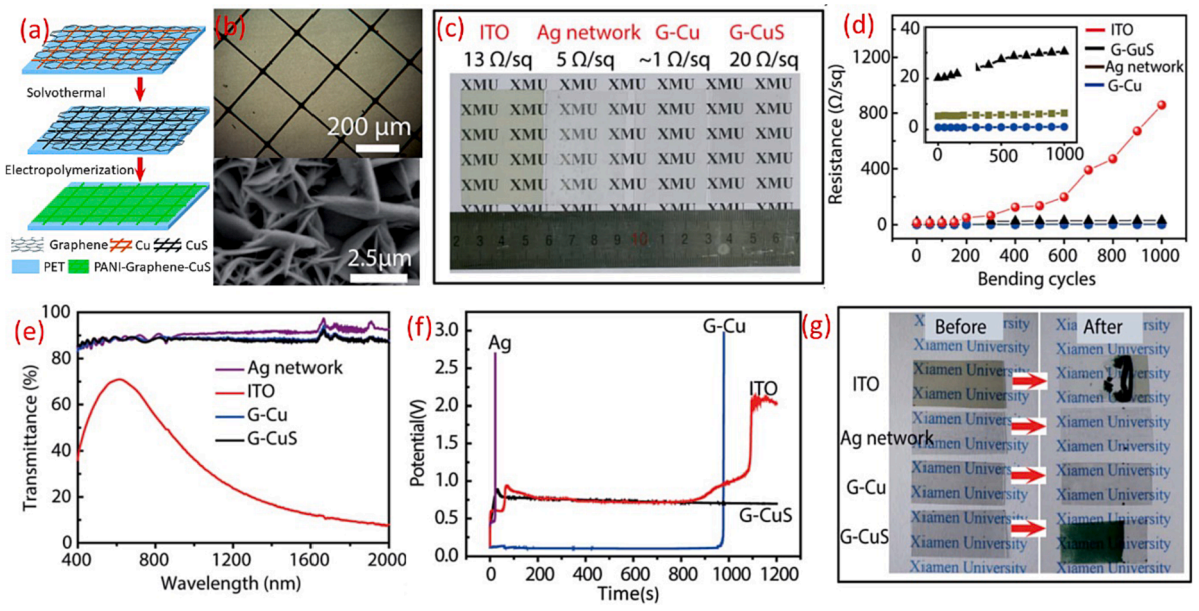

Fig. 7. (a) Solvothermal and electropolymerization reactions for synthesizing G–CuS/PANI on the PET substrate. (b) Scanning electron microscopic image of G-CuS network. Comparison of performances of various properties of G-Cu, G-CuS, Ag network and ITO transparent flexible electrodes including (c) electrical properties (d) resistance variation under mechanical bending (e) optical transmittance (f) chemical stability through chronoamperometry study and (g) deposition of PANI film via electroplymerization. (a-g) Reproduced from Ref. [51] with permission from the Royal Society of Chemistry.

till 9000 bending cycles) properties [90]. Coating of a similar electrochromic polymer (PANI) on the top of the PANI-CNT/ITO electrode shows greater performances due to the intimate interface of the material which exhibits excellent electron transfer [90]. It was found that after cyclic bending PANI deposited on ITO/PET suffers from delamination issues as compared to PANI coated on PANI-CNT/PET [90]. Similar to polymer based current collectors and substrates for a flexible wearable application, fibre based substrates have attracted significant attention for energy storage device fabrication due to their flexibility, strong hydrogen bond with active materials and mechanical reliability [53]. However, achieving transparency in fibre devices is very easy to obtain for an EESD. This issue was overcome by utilising ultra-thin carbon nanofibres (CNFs) as a substrate by controlling the CNF density during preparation. The CNF has a diameter of about 20 nm and without any electrodes it shows transmittance of 99.1 % [53]. Further Ag NW network coated on this CNF will be act as cc/substrate with transmittance of 89.0 % and 18 sq. Ω^{-1} sheet resistance [53].

As an alternative to ITO or metal NWs, another transparent electrode material option is metal sulphides. As an example, CuS is one of the competitive metal sulphide materials used for the fabrication of transparent electrodes [51]. However, its continuous film structures show low transparency (~60 %) and high sheet resistance limiting its application in EESDs. It was reported that to obtain high transparency and low sheet resistance, converting a continuous thin film into a mesh structured with random or periodic lines was highly advantageous. Fig. 7**a** shows the schematic representation of the coating of PANI and graphene on the top of the CuS which leads to form a high conductive continuous film. The major advantage of this coating is that it will protect the metal from oxidation and such electrodes are applicable to flexible and stretchable EESD fabrication. Recently one report on graphene coated CuS networks on a PET sheet (G-CuS/PET) (microscopic image shown in Fig. 7b) demonstrated a low sheet resistance and high transmittance cc/substrate for the fabrication of a flexible EESD [51]. The authors carried out a detailed comparative study (electrical, optical, mechanical and chemical stability) of various transparent electrodes for the potential fabrication of flexible EESDs. Fig. 7c shows a comparison of sheet resistance for various electrodes including ITO, Ag network, G-Cu and G-CuS [51]. The metal coated with graphene shows the lowest sheet resistance. The mechanical flexibility studies given in Fig. 7d confirm that ITO suffers from degradation of the material after multiple bending cycles. For visible light, the Cu network shows transmittance of 93.4 % and it was found that the wrapping of graphene reduces the transmittance (e.g., for G-Cu 88.1 % and G-CuS 88.3 %). As compared to the other three electrodes, ITO shows the lowest transmittance, in particular a significant drop in infrared transmittance as reported in Fig. 7e [51]. Even though the Ag network and G-Cu collectors show excellent electrical and optical properties, the chemical stability of these electrodes was poor. Ag networks are stable for 20 s and G-Cu shows up to 960 s stability due to graphene wrapping. ITO also shows poor chemical stability against corrosive salts and acids. On the other hand, G-CuS shows better stability and is suitable for deposition of PANI films during electro polymerization (Fig. 7f and 7 g) [51]. Further, G-CuS is stable to thermal oxidation at 160 °C, humid air (80 % relative humidity at 85 °C), and H_2O_2 solution [51]. These studies show that for flexible EESD fabrication G-CuS/PET could be one of best cc/substrates and deposition of this on PDMS or ecoflex substrates allows stretchable EESD development. Further studies will be required to enhance the transparency above 90 % and reduce the sheet resistance. For future cc/substrate development, the flexibility of the EESD purely depends on the type of material and among the various electrodes conjugated polymers such PANI and PEDOT:PSS shows excellent electrochromic and energy storing performance [90,99,100].

4.2. Study on electrolytes used for flexible and stretchable EESD

The high-performance of ESCs and ECBs depends on gel, liquid and solid state electrolytes [101]. The most relevant requirements for electrolytes are a high operating potential window, long lifecycle, and fast optical modulation in an EESD. This results in the need for (i) high ionic conductivity, (ii) high electrochemical, mechanical and thermal stability (under ultraviolet irradiation) (iii) suitable elastomeric and adhesive properties [102,103]. When considering the fabrication of flexible EESDs using liquid electrolytes, solvent evaporation under dry room environments or in ambient air and electrolyte leakage due to mechanical deformation are the major problems [53]. To overcome this, gel electrolyte and solid electrolytes were tested for EESD development which showed improved flexibility without leakage. However, the lack of ionic conductivity (1–50 mS. cm^{-1}) and narrow operation voltages are the main problems in gel and solid electrolytes as compared to liquid electrolytes [37]. Currently, most studies of solid or gel electrolytes are focussed on enhancing the ionic conductivity. Among the electrolytes studied, polymeric gel electrolytes offer high performance for EESDs [37]. For example, polyacrylamide (PAAm)-based hydrogel electrolyte with LiCl salt have high dehydration resistance, high ionic conductivity, and operate in a wide potential window (0–2.4 V) even after 16 days of exposure to ambient conditions [37]. This transparent stretchable gel electrolyte shows high ionic conductivity (265 mS. cm^{-1}) as well as stretchability of up to 80 %. For measurements after 16 days (30 % humidity), the electrolyte exhibited 94 % of its ionic conductivity (in the range of 265 to 249 mS. cm^{-1}) and 93 % water content. An EESD based on this electrolyte was operated for 50,000 charging discharging cycles at an operating potential of 0–2.4 V with 92.9 % capacitive retention. In addition, low dehydration of PAAm based gel electrolytes in an operating potential of 5 V showed that the EESD could be operated at 2 V for a long period of time [37]. A gel electrolyte (CN:PC:PMMA:$LiClO_4$ was 70:20:7:3 wt%) based on poly(methyl methacrylate) (PMMA) with $LiClO_4$ salt dissolved in acetonitrile (ACN) as a solvent, and propylene carbonate solution as the plasticizer behaves as an excellent transparent electrolyte with 96.2 % retention in transmittance (after 14 days in air atmosphere) and operating voltage 0 and 2.5 V [53]. This type of electrolyte will be advantageous for applications such as sensors and related components working at potentials below 2.5 V. A recent study shows that multifunctional hydrogels have advantages in reducing the structural and technical complexity in EESD fabrication, including the enhancement of the overall transmittance by reducing the number components [104]. Recently, a multifunctional hydrogel synthesized from LiCl and acrylamide were used for flexible EESD fabrication. These devices show optical contrast (35 %), high ionic mobility and faster response speed (colouring 1.6 s, fading 2 s) [104]. These electrolytes, along with PEDOT: PSS and Ag nanowire electrodes shows large areal capacitance (0.58 mF. cm^{-2}) [104]. To overcome the issues of electrolyte displacement during bending of the EESD device, the trapping of

electrolyte ions (Al^{3+}) in the pores of the flexible separator AGM in Al_xWO_3 based flexible ECB is a promising method.

4.3. Electrochromic materials

To date, several materials have been used as electrochromic materials for ESC and ECB fabrication. These include transition MO_x, conducting polymers, inorganic–organic composites and bimetallics or alloys. It was found that there is a limited subset of materials used for the fabrication of flexible and stretchable EESDs, as discussed in the following sub sections. The electrochemical and electrochromic properties of flexible EESDs depends on the type of the electrodes used for their fabrication.

4.3.1. Metal oxide based flexible EESD

The metal oxides shows both cathodic and anodic electrochromic performances. In MO_x the intercalation/de-intercalation of electrolyte ions causes the electron exchange between the different positions of metal states in MO_x, which leads to colour changes [46,103,105]. The high pesuodocapacitance of the MOx leads to high specific capacity of the material. Due to these unique electrochromic and electrochemical properties EESD using MO_x demonstrated excellent performances [46,103,105]. In this section we provide a detailed discussion on various MO_x used for the fabrication of flexible EESDs.

Preparation of the transition MO_x film in a flexible substrate through low temperature processing is challenging. For achieving low temperature processes for flexible EESDs, a detailed investigation in MO_x powder preparation and its film fabrication methods are

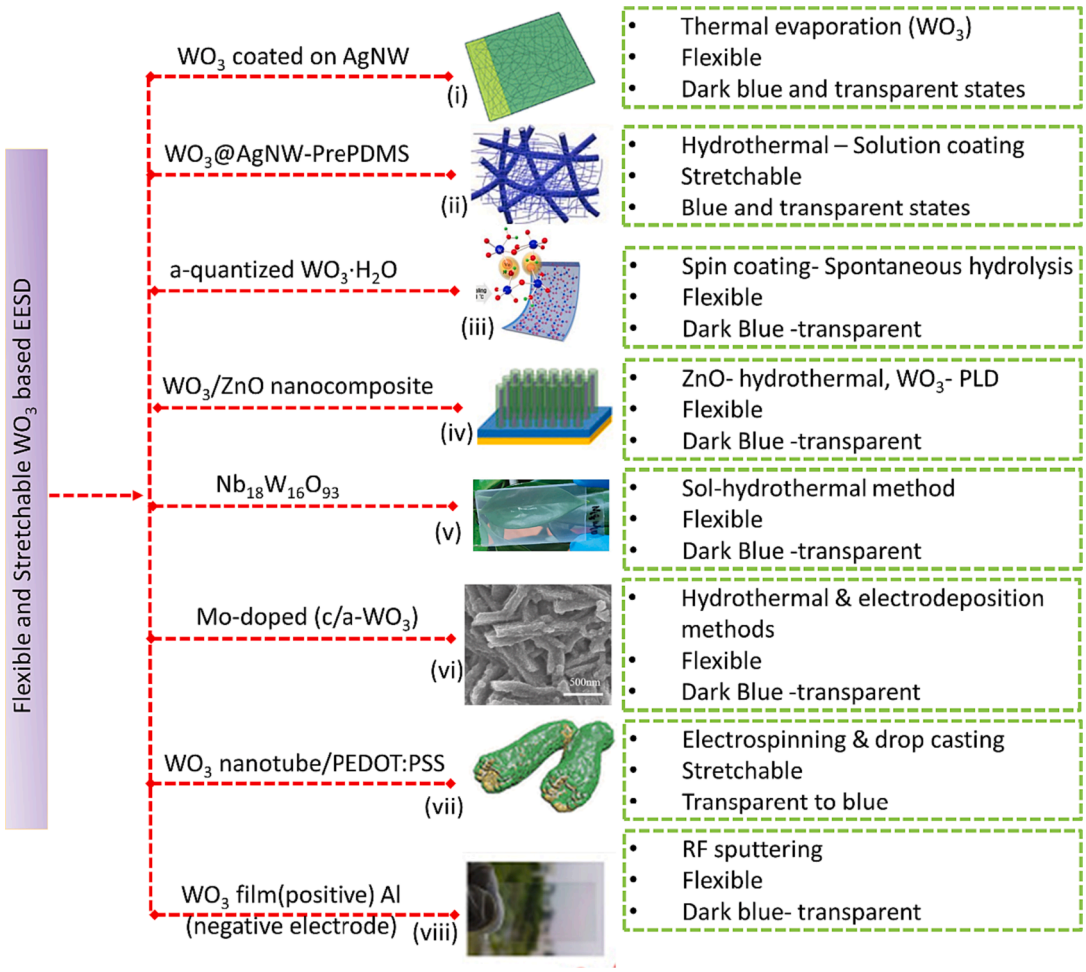

Fig. 8. Summary of WO_3 based flexible and stretchable EESD and its fabrication method (i) WO_3 coated on AgNW, Reproduced from Ref. [75] with permission from the Royal Society of Chemistry. (ii) WO_3@AgNW-PrePDMS. Reprinted from Publication [87] Copyright (2021), with permission from Elsevier. (iii) Amorphous quantized $WO_3{\cdot}H_2O$ Reprinted from Publication [52] Copyright (2021), with permission from Elsevier. (iv) WO_3/ZnO composites. Reprinted from Publication [110] Copyright (2021), with permission from Elsevier. (v) $Nb_{18}W_{16}O_{93}$ film. Reprinted (adapted) with permission from. [118]. Copyright (2021) John Wiley and Sons. (vi) Mo-doped (c/a-WO_3). Reprinted from Publication [56] Copyright (2022), with permission from Elsevier. (vii) WO_3 nanotube/PEDOT:PSS. Reprinted (adapted) with permission from [37]. Copyright (2019) American Chemical Society. (viii) WO_3 film. Reprinted from[86] Publication Copyright (2020), with permission from Elsevier.

necessary. The MO_x powders or inks are mainly prepared by using hydrothermal, sol gel [106], solvothermal method [107,108], co-precipitation [106]. For a MO_x nano materials preparation, hydrothermal approach is one of the most suitable method especially for fine tuning the size and shape of the materials [109]. There are many materials including WO_3, and ZnO were prepared by hydrothermal synthesis method for the fabrication of flexible EESD [87,110]. In the solvothermal method, aqueous and non-aqueous solvents were used for the preparation of MO_x films. This method enables the control of the crystalline phase, shape and size of the material and its properties may be controlled by varying the solvent, surfactant, precursors, reaction time and temperature [111]. For example, to prepare a $NiMoO_4$ nanosheet based electrochromic energy storage film, different solvents including (i) pure ethylene glycol (ii) ethylene glycol with water (iii) and solvent of pure water were investigated [107]. For flexible $W_{18}O_{49}$ NWs film for IR electrochromic device fabrication, $W_{18}O_{49}$ NWs were prepared by the solvothermal method and the film deposited using spray coating [108]. Co-precipitation is another method used for MO_x film synthesis. In this method the reduction of metallic ions occurs at low temperature in a basic solution [106]. It provides high purity MO_x particles, high yield, easily reproducible approach, and low cost. However, the processing temperature, pH and ionic strength and type of basic solution depends on the preparation of the powder [106]. For the fabrication of bendable and twistable oxide-polymer electrochromic films, WO_3 was prepared using this approach and the prepared powder was coated on a PET substrate using drop casting [112].

When we consider flexible electronic technology, currently, inkjet and screen printing are considered attractive and efficient techniques for the direct fabrication of functional material thin films onto flexible substrates including plastic foils, paper or rubber. This is attributed to their simple and solution-based processing at a low-temperature, low-cost, higher adaptability for large scalability, and avoidance of high-vacuum conditions [113,114]. The inkjet printing technique dramatically increases manufacturing process as compared to conventional microfabrication which involves multistage photolithography and deposition. The most commonly used inks for active materials in inkjet printing comprise of metal nanoparticles, and organic polymers as well as carbon materials such as NW, CNT and graphene. For instance, a combination of techniques including inkjet printing and sol–gel synthesised hydrated WO_3 and VO_x nanoparticles have been developed to fabricate flexible electrodes for solid-state electrochromic films [115,116]. These methods are well reported for flexible electronic devices and electrochromic layer fabrication. Moreover, when considering MO_x film fabrication, various chemical and physical deposition methods have been implemented. The mechanism for the operation of some of these methods were summarised in [117]. In which some of the methods include spin coating [52], thermal evaporation [75], pulse laser deposition [110], electrodeposition [56], electrospinning and drop casting [37], RF sputtering [86] and spray coating [108] are used for flexible EESD fabrication. A summary of different methods of fabrication for WO_3 based flexible EESDs is given in Fig. 8. It was observed that, the well-known spin coating, electrochemical deposition and evaporation methods of fabrication leads to delamination issues in film development and poor adhesion [87]. This leads to a decrease in the performance of EESDs. One of the approaches to overcome these issues are the partial embedding of the electrochromic material on the stretchable substrate [87].

Among the various transition MO_x, WO_3 has emerged as one of the best cathodic materials for EESD development due to their good electrochemical, electrochromic properties and potential in manufacturing of flexible devices [55–57]. In WO_3 based EESDs, during the electrochemical reaction with the intercalating of metal cation, W^{6+} is reduced to W^{5+} and W^{4+}. This reduction processes leads to a colour change from colourless to blue [54]. Studies reveal that, the crystalline structure and fabrication method contributes significant differences in electrochemical and electrochromic properties of the flexible EESD based on WO_3. In the first report of a flexible WO_3 based ESC, the electrodes were fabricated by using Ag NW/WO_3 hybrid films. The authors explained that due to the H^+ insertion and extraction process on the electrode, the colour of the AgNW/WO_3 electrode can reversibly change between dark blue (11.8 % at 633 nm) and transparent states (55.9 % at 633 nm) [75] as shown in Fig. 9**a**. The fabricated ESC shows capacitance of 13.6 mF. cm^{-2}, and (138.2F. g^{-1}) at 10 mV. s^{-1}. The high conductivity of the AgNW coated on PET/PDMS substrate (by spin coating) and the compact contact between the cc/substrate with WO_3 results in this ESC having a high colouration time (T_c – 1.7 s) and corresponding bleaching time (T_b –1.0 s) [75]. The observed performances are comparable with devices based on nickel oxide nano flake glass (T_c-2.7 and T_b-1.8 s) [119] and silver-decorated WO_3 film (T_c- 3.9 and T_b – 3.2 s) [120]. One of the major issues of layer-by-layer coating of active

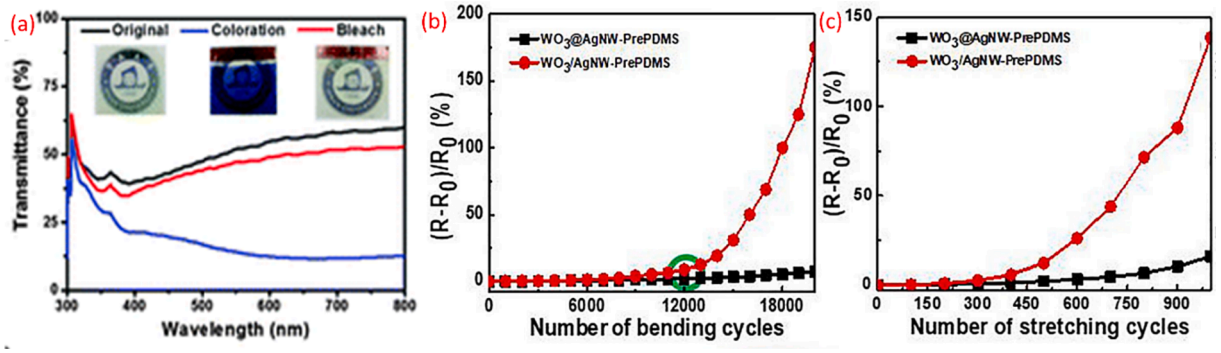

Fig. 9. (a) Transmittance spectra and images of the Ag NW/WO_3 electrode measured under different voltage conditions. Reproduced from Ref. [75] with permission from the Royal Society of Chemistry. (b) and (c) Comparison of resistance variation during bending and stretching for WO_3@AgNW-PrePDMS and WO_3/AgNW-PrePDMS electrodes. (c and b) Reprinted from Publication [87] Copyright (2021), with permission from Elsevier.

electrodes on a flexible substrate is its delamination during multiple bending. Increasing the thickness for enhancing the conductivity and adhesion of the AgNW is not suitable due to its reduction of transmittance. Recently, issues related to delamination of the electrodes were resolved by developing WO_3@AgNW core–shell NW embedded in the PDMS substrate (WO_3@AgNW-PrePDMS) [87]. The embedding of material on the PDMS helped to strongly integrate each layer and protect the AgNW from oxidation, which enhanced the stability of the device. When the authors compared the bending performances, they found that after 20,000 bending cycles (0. 8 cm radius), the relative change in resistance was increased to 175 % for WO_3/AgNW-PrePDMS but for WO_3@AgNW-PrePDMS the value was 8.3 %. The significant variation of the resistance of WO_3/AgNW-PrePDMS is due to delamination of material after 12,000 cycles as shown in Fig. 9b [87]. In addition to the bending analysis, the stretching (1000 cycles at 70 % strain) of the WO_3@AgNW-PrePDMS (resistance variation 14 %) gives better performances compared to WO_3/AgNW-PrePDMS (resistance variation 138 %) as given in Fig. 9c [87]. The energy and power density of these embedded materials needs to be further studied along with their application for powering wearable electronics.

The hydrolysis effects on sol–gel coated films are one of the promising methods to develop flexible EESDs. Such methods of

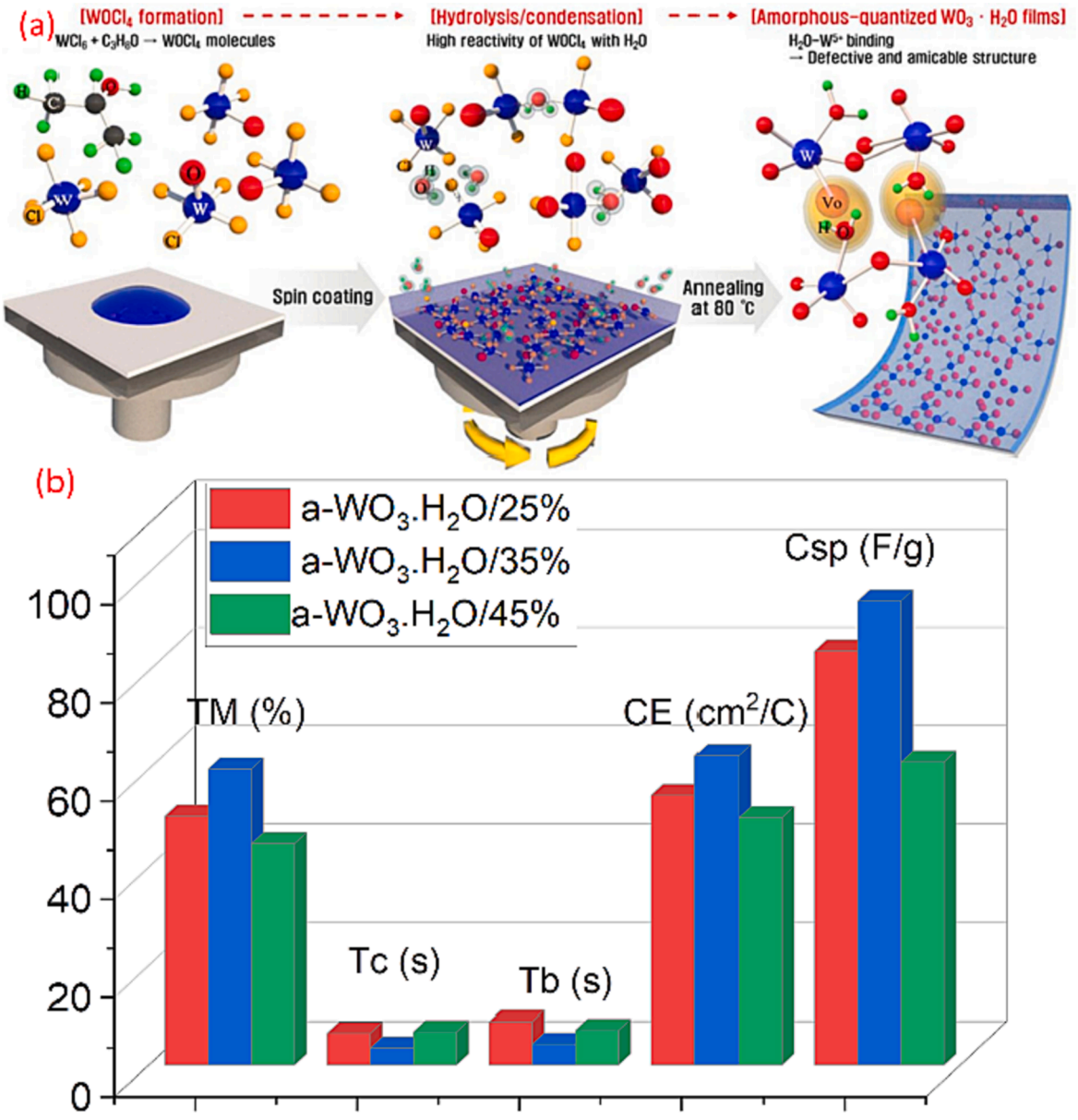

Fig. 10. (a) Schematic illustration of mechanism of development of the a-quantized $WO_3{\cdot}H_2O$ films. Reprinted from Publication [52] Copyright (2021), with permission from Elsevier. (b) Electrochemical and electrochromic properties of a-$WO_3{\cdot}H_2O$ in different humidity level. (TM- transmittance modulation, T_c- colouration time, T_b- bleaching time, CE- colouration efficiency, C_{sp}: specific capacitance).

fabrication, especially at low temperature (<100 °C) and low cost have significant advantages especially for large scale production of flexible EESDs. For example amorphous $WO_3{\cdot}H_2O$ (a-$WO_3{\cdot}H_2O$) films, synthesised via accelerated hydrolysis effects during spin-coating can be annealed at low temperature 80 °C (shown in Fig. 10**a** [52]). The hydrated phase of this amorphous film has high porosity and oxygen vacancies for increasing the electron density to improve the electrochemical performances [52]. It was observed that the intercalated water molecules in crystalline WO_3 structures can form infinite 2D layered structures with expanded gaps between the stacks, leading to rapid diffusion of ions in the electrolyte to improving the ionic storage ability [121]. The oxygen vacancies and porosity were achieved through hydrolysis of $WOCl_4$ molecules with H_2O via controlled humidity changes during spin coating of the WCl_6 solution [121]. The increased aggregation of amorphous clusters, and intercalation of water molecules leads to abundant porosity and oxygen vacancies in the film. The increasing nucleation and aggregation rates of amorphous film with humidity could be observed through the microscopic images. It was found that film shows a porous structure at 35 % of humidity and increasing the humidity leads to cracking of the film. Moreover, the X-ray photoelectric spectroscopic (XPS) analysis of this material confirmed that, the oxygen vacancy in 35 % humidity treated film provided extra electrons and efficient charge transport channels for electrochemical reaction. The electrochemical and electrochromic performances of $WO_3{\cdot}H_2O$ in different humidity level is given in Fig. 10b and data to draw this figure were extracted from the Table in the work [121]. This study shows that, while reacting with $LiClO_4$/PMMA/PC-based gel polymer electrolyte, the increase in Li ion capacity due to electrochemical active sites and shortened Li ion diffusion pathways for the porous film results in improved transmittance modulation and specific capacitance. Moreover, the abundance of oxygen vacancies increases the electrical conductivity for the electrochemical reaction and fast switching speeds [121].

In addition, with dense or nanostructured WO_3 films for EESDs, the binary oxide has also demonstrated significant influence, enhancing the electrochemical properties, storage capacity and CE of the device. In one of the reports, by using combined hydrothermal (for growing ZnO nanowire) and pulse laser deposition (PLD) (for WO_3 deposition) WO_3/ZnO nanocomposite films (shown in Fig. 11**a**) were prepared which have high storage capacity due to larger degrees of Li^+ intercalation[110]. Here the ZnO provides a porous template and high surface area for the deposition of WO_3. When compared with dense WO_3 films (Fig. 11b (i)) the active sites for redox reaction in WO_3/ZnO is very high (as shown in Fig. 11b (ii)), reducing the diffusion paths for Li ions[110]. This results in high current densities for WO_3/ZnO nanocomposite EESDs as compared with WO_3 based EESDs, as shown in the CV plot in Fig. 11c. The observed enhanced electrochemical and electrochromic performance of these devices is shown in Table 1. In addition to binary oxide composite, it was also noted that the unique structural and electronic properties of bimetallic electrodes from such oxides leads to excellent EESDs. Another bimetallic oxide based flexible EESD was fabricated using $Nb_{18}W_{16}O_{93}$ films [118]. Even though WO_3, exhibits excellent electrochemical and electrochromic performance, the reversibility of the electrochromic performance is

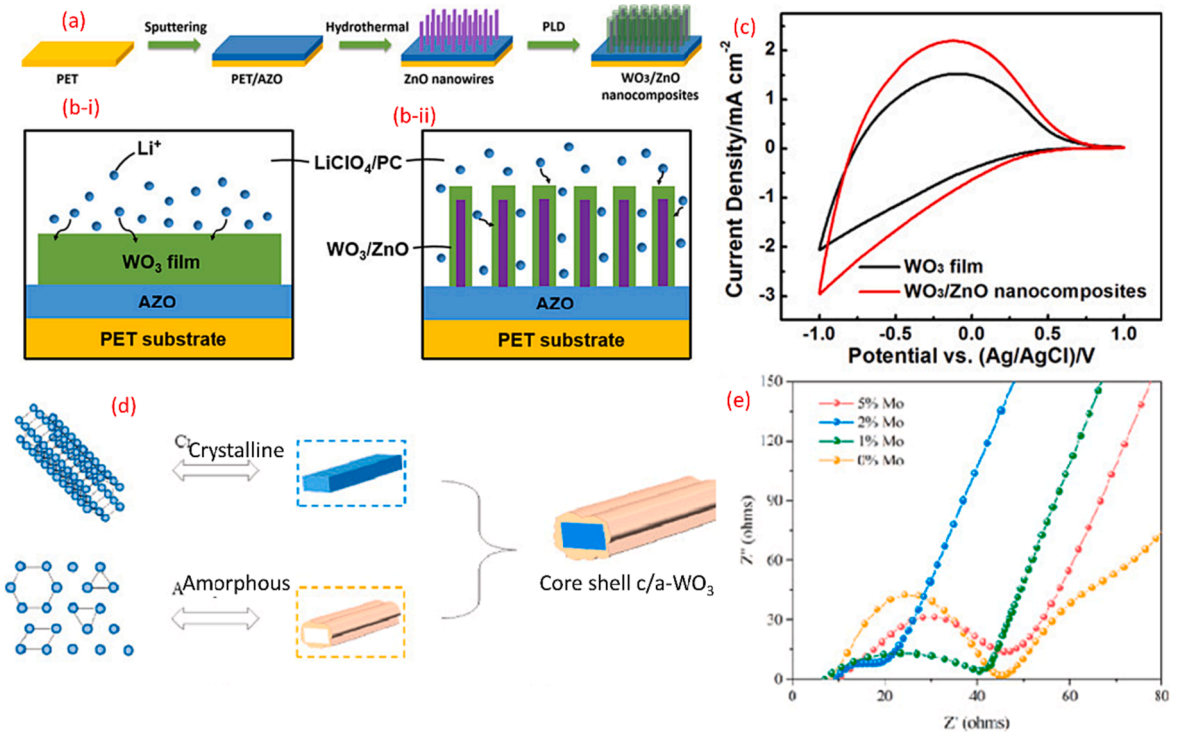

Fig. 11. (a) Schematic illustration of development of WO_3/ZnO nanocomposite for EESD (b) Model of insertion/extraction of Li^+ in WO_3 and ZnO based structures. (c) Comparison of CV curve for WO_3 and WO_3/ZnO nanocomposite. (a-d) Reprinted from Publication [110] Copyright (2021), with permission from Elsevier. (d) Schematic illustration of assembly of c/a –WO_3 formation (e) The EIS analysis, which represented as a Nyquist plot for c/a-WO_3 film for various Mo doping to enhance the electrochemical activity. (d and e) Reprinted from Publication [56] Copyright (2022), with permission from Elsevier.

comparatively poor due to partial Li ion trapping in the WO_3 lattice[118].

Though Nb_2O_5 exhibits excellent reversibility of its optical properties, in the coloured state the film exhibits poor colouration. The bimetallic oxide of WO_3 and Nb_2O_5 overcomes this issue due to its combined chemical properties. As compared to 53.8 mA. h. g^{-1} (at 2.1 A. g^{-1}) and 70.3 mA. h. g^{-1} (at 2.3 A. g^{-1}) for WO_3 and Nb_2O_5 based EESD electrodes, the $Nb_{18}W_{16}O_{93}$ based film exhibits a storage capacity of 151 mA. h. g^{-1} (at 2 A. g^{-1}) [118]. This excellent electrochromic and electrochemical performance highlights the promise for the application of $Nb_{18}W_{16}O_{93}$ films for flexible EESDs. $Nb_{18}W_{16}O_{93}$ have been demonstrated in flexible large window based EESDs in combination with a NiO cathode electrode [118].

In addition to binary MO_x for enhancing the performances of EESDs, recently it was reported that metal doping will also enhance device properties due to the structural distortion caused by the doping elements. A Mo-doped crystalline/amorphous WO_3 (c/a-WO_3) film was developed by combined hydrothermal and electrodeposition methods for flexible EESDs, as shown in Fig. 11d [56]. The similar atomic structure of Mo and W are advantageous for such doped film synthesis and development. In another work, it was found that the structure a-WO_3 and c-WO_3 and Mo doping levels influenced the electrochemical and electrochromic performance of the device [56]. The low internal resistance and fast charge transfer of a- WO_3 films is suitable for the effective oxidation/reduction of c/a-WO_3 and enhance ion storage. Moreover, the a -WO_3, giving faster switching speed (T_b – 7 s and T_c – 9 s) than c-WO_3 (T_b- 15 s T_c –20 s). Hence switching times of c/a-WO_3 are faster than c-WO_3. Further, varying Mo- doping results in large variations in the c/a –WO_3 film charge transfer resistance and is given in Fig. 11e. This leads to a change in the electrochemical activity [56]. The observed performance of the device is given in Table 1.

4.3.2. Polymer based flexible/stretchable EESD

The rich colour change, fast response time, high flexibility, low temperature processing, and ease of fabrication enable conducting polymers to be realise better flexible ESSDs as compared with MO_x based devices. In a conducting polymer based EESD, the electrochromic performance is due to the oxidation of electrons in the material in which charge transfer takes place through the conjugated main chain [46,103,105]. During charging the carrier transport and polarity of the conjugated polymer will change [46,103,105]. PANI, polypyrrole (PPy), PEDOT:PSS and polythiophene (PTh) are the main conducting polymers used for EESD fabrication [100]. Conducting polymers can overcome the material cracking during bending which is normally observed in MO_x based flexible EESDs. The electrochromic performance of different polymers is distinct and has been recently summarised [100]. Among the various conducting polymers PANI has been identified as one of the best electrochromic materials for flexible EESD fabrication due to its facile synthesis, rich colour changes, high capacitance, high energy storage performance, and better stability [71,122,123]. Nanostructured PANI electrodes exhibit excellent ion diffusion in electrochemical devices. For example PANI NW vertically aligned on PEDOT:PSS/PET based flexible electrodes show 60 % transmittance at the wavelength of 500 nm [123]. A fully flexible ESC as shown in Fig. 12**a** exhibits a transmittance of 30 % its comparison is given in Fig. 12b and 0.017F cm^{-2} (400F. cm^{-3}) capacitance at 5 mV. Such PANI NW

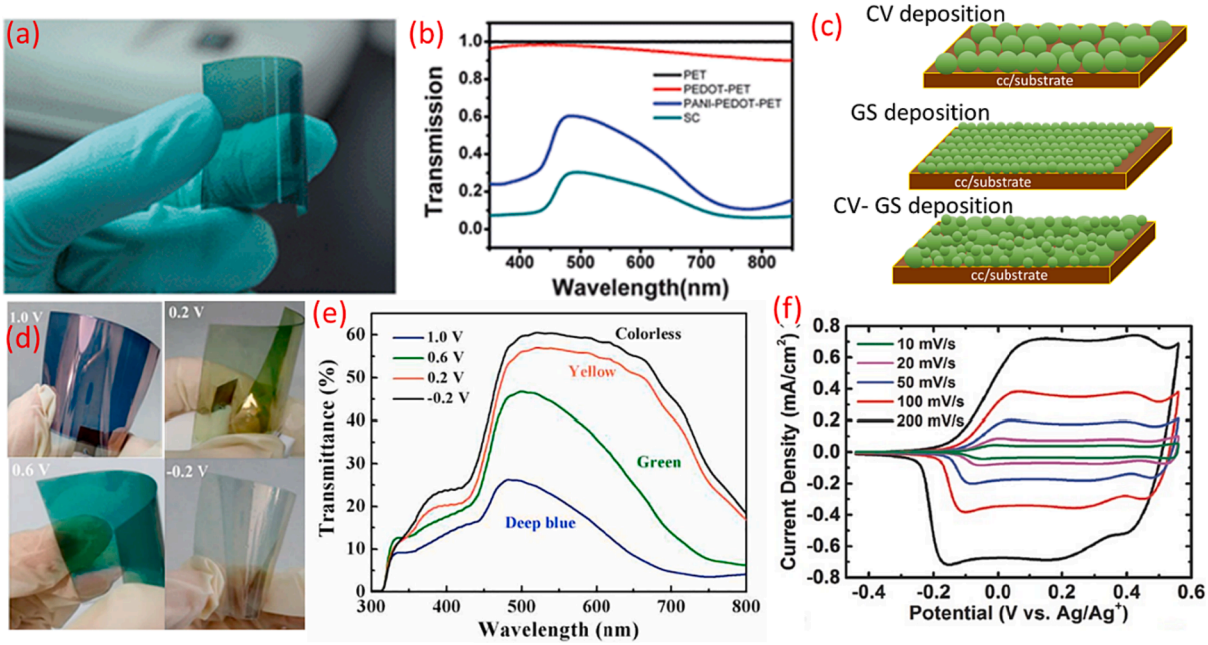

Fig. 12. (a) Image of PANI + PEDOT:PSS based ESC with transmission of 60 % at the wavelength of 500 nm [123]. (b) The comparison of transmittance of different films [123]. (c) Schematic illustration of CV-GS technique for the preparation of loose and porous PANI electrode (d) and (e) Image and transmittance spectra of PANI film coated by CV-GS in different oxidation state. Reprinted from Publication [71] Copyright (2018), with permission from Elsevier (f) CV curve of PBOTT-BTD film in different scanning rate. Reprinted (adapted) with permission from [124] Copyright (2016) John Wiley and Sons.

electrodes exhibit a light-yellow green colour when the device is discharged to 0 V and the device shows a deep blue colour for 1 V charging. The flexibility studies of this ESC show that even after 200 cycles of bending the capacitance is almost the same [123]. PANI films may be easily prepared by chemical and electrodeposition methods. In a recent study authors observed that instead of compact structured films, loose and porous nanoparticle based PANI films have a better energy storage performance due to surface interactions, a high surface area of nanoscale dimensions, and penetration of ions from the electrolyte to the electrodes, along with mitigation of the ill effects of mechanical deformation [71]. Such nanoparticle based loose and porous PANI electrodes could be prepared by combined CV (which allow to make loose, larger size and irregular structure of the material) and galvanostatic (allow to form compact, small size uniform nanostructures) (CV-GS) techniques of electrodeposition as shown in the Fig. 12c [71]. CV-GS coated PANI films show a response time (time required for 90 % change in the full oxidation or reaction state) of 3.90 s for oxidation and 2.61 s for reduction reactions. This fast response of the film reveals the benefits of ion intercalation/deintercalation [71].

The rich colour changes in the PANI film are due to its oxidation state (shown in Fig. 3d). PANI shows three major oxidation states such as (i) the fully reduced leucoe meraldine (LB) form (ii) the 50 % oxidized emeraldine salt (ES) form and (iii) fully oxidized pernigraniline (PS) form. In the LB form it exhibits a transparent yellow colour, ES leads to a green colour and in the PS form it is a purple colour as shown in Fig. 3d and 12d [71]. The corresponding transmittance spectra is shown in Fig. 12e [71]. As can be seen from Fig. 12d, with the potential scanning from 1.0 V to − 0.2 V, the colour of the film transforms from deep-blue to blue, green, yellow or colourless. Hence the charge density of the device decreases when sweeping between −0.2 V to 1 V. Total charge density as a function of bias and the films corresponding colour are shown in Fig. 3b and 3c revealing the excellent electrochromic energy storage performance of the PANI based devices [71]. The specific capacitance and electrochromic performances are provided in Table 1.

In conjugated polymers for EESD design another type of polymer which shows excellent electrochemical redox properties are donor–acceptor (D–A) conjugated polymers. In such materials the electron donor and acceptor building blocks can be selected and tuned. Among these Poly[4,7-bis(3,6-dihexyloxy-thieno[3,2-b]thiophen-2-yl)]-benzo[c][1,2,5]thiadiazole (PBOTT-BTD) shows pseudocapacitive D–A polymers with specific capacitance of 2.5 mF. cm^{-2} (31F. g^{-1}) at a current density of 0.1 mA. cm^{-2} [124]. This

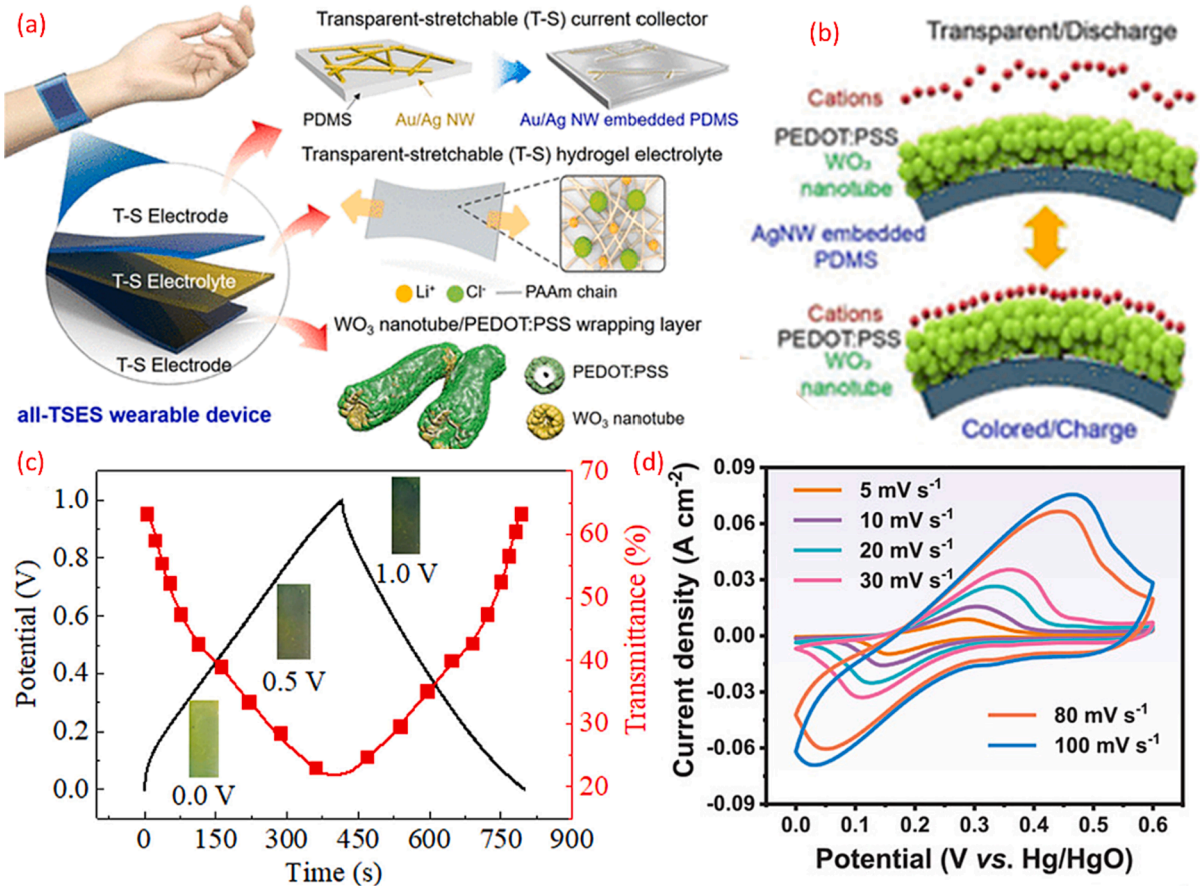

Fig. 13. (a) Schematic illustration of the wearable transparent stretchable EESD using WO_3 nanotube/PEDOT:PSS based electrode. (b) Ions distribution during charged and discharged state of WO_3 nanotube/PEDOT:PSS based EESD. (a-b) Reprinted (adapted) with permission from [37] Copyright (2019) American Chemical Society. (c) Charging discharging and transmittance of P5ICN/WO_3 based device. Reprinted from [125] Publication Copyright (2021), with permission from Elsevier. (d) CV curves of the 3D NM@NiCo BH for different scan rate. Reprinted (adapted) with permission from [96] Copyright (2021) John Wiley and Sons.

PBOTT-BTD film appears green and blue colour during its uncharged (−0.4 V) and charged (0.6 V) state, respectively[124]. The CV analysis of the PBOTT-BTD shows its good redox reversibility during charging and discharging in a wide potential window, as shown in Fig. 12f [124]. The high energy storage performance of the material is thus demonstrated. Further studies on this material combined with an MO_x or conjugated polymers will be beneficial for flexible EESD applications.

4.3.3. Composite material or organic–inorganic materials based flexible EESD

In comparison with pure MO_x or polymer based EESDs, it was noted that due to synergetic effects, hybrid composite based materials may exhibit excellent performance in flexible EESD. For example, in WO_3 based flexible EESDs, the delamination issue during cyclic bending could be overcome via coating with conducting polymer films. This was successfully proved through coating of PEDOT: PSS film on the top of WO_3 nanotube which was electrospun on the Ag NW current collector [37]. The developed WO_3 nanotube/PEDOT: PSS based EESD shows potential implementation for wearable system. The schematic representation of the EESD is given in Fig. 13**a** [37]. During electrochemical reaction (the GCD shown in Fig. 13b) both WO_3 nanotubes and PEDOT: PSS undergo cathodic colouration (from transparent to blue) and hence enhances both colouration efficiency (20.4 % to 83.9 cm^2. C^{-1}) and energy storage properties (specific capacity improved by 38.6 % to 471.0F. g^{-1}) compared to pristine WO_3 nanotubes (the performances given in Table 1) [37]. Another hybrid material which shows excellent electrochromic and electrochemical property is WO_3 (cathode colouring) and poly (5-cyanoindole) (P5ICN) (anodic colouring) [125]. For a current density of 2 mA. cm^{-2}, P5ICN/WO_3 hybrid material shows a specific capacitance of 89.2 mF. cm^{-2}[125]. The authors observed that the specific capacitance of this hybrid composite is much higher than that of other composite electrodes including $W_{18}O_{49}$/PANI (10 mF. cm^{-2}) [126], PICA/TiO_2 nanocomposites (23.34 mF. cm^{-2}) [127], silver nanowire/WO_3 (13.6 mF. cm^{-2}) [75], WO_3/ZnO (15.24 mF. cm^{-2}) [110] and PEDOT:PSS)/PANI (17 mF. cm^{-2}) [123]. This P5ICN/WO_3 exhibits 91 % of the initial specific capacitance after 3000 cycles. In their neutral states, the colour of P5ICN is yellow and for WO_3 is colourless (due to out of H^+ ion). Hence, the device colour is dominated by the yellow colour of P5ICN [125]. However, during chemical reaction, the colour of the composite P5ICN/WO_3 is blue-green due to the combination of blue and yellow. It was found that during charging from 0 V to 1 V the transmittance of the device decreased from 64 % to 22 %, and the colour of the device varies as shown in Fig. 13c. Hence, the energy state of the EESD could be predicted using its colour and transmittance. At an optical contrast of (95 %), the T_b and T_c of the P5ICN/WO_3 were 2.06 s and 1.38 s [125]. The CE of the device found to be 548 cm^2. C^{-1} and is higher due to the synergetic effects of the composite material [125]. A further study on this material with flexible ITO or Ag NW based cc/substrates will be promising for flexible EESD fabrication for operating high energy density device applications.

For flexible EESD fabrication, high specific capacity materials with ultralight weight electrode architectures and long-term stability will be advantageous. The material properties, including the abundance of oxygen vacancies, tuneable composition, and high CE will strongly influence the device performance. Moreover, eco-friendly binderless fabrication methods will lead to the development of highly functional EESDs [96]. With regard to fabrication, as compared to physical deposition methods (sputtering, printing, thermal evaporation), the electrodeposition method ensures uniform film thickness and composition and avoids high temperature processing. Moreover, the substrate used for deposition and the electrodeposition bath are recyclable, making it both cost effective and eco-friendly. Through this method, transition bimetallic hydroxide, which has a high theoretical capacity, can easily be deposited on designed patterns. Recently, Ni-Co bimetallic hydroxide (NiCO-BH) deposited on a 3D NM current collector via combined photolithography and electrodeposition [96] has demonstrated an aerial capacity of 68.61 μA. h. cm^{-2} at 1 mA. cm^{-2}. The CV curve of the material exhibits battery characteristics (shown in Fig. 13d) and hence the device shows high capacity (37.78 μA. h. cm^{-2}), even at a high current density (20 mA. cm^{-2}). The high energy density (75.58 μA. h. cm^{-2}) and power density (51.46 μW. h. cm^{-2}) with 83.7 % capacity retention after 15 000 cycles (at 10 mA. cm^{-2}) reveals high performance for wearable applications. When fully charged (1.434 V) the devices are blackish green and while discharging, the colour of the EESD gradually faded. Once fully discharged the device turned to a brown colour. This colour change can provide a visual cue to the charge status of the energy storage device. The high performance of this NiC BH is due to its excellent electrochemical activity and multiple redox chemical reactions [96]. Along with composite materials or layered electrodes, asymmetric or hybrid electrodes in EESD design exhibit excellent performance, especially for electrochromic materials with matching thermodynamic and kinetic properties [85]. A flexible ECB was designed using Zn//PPy electrodes on ITO coated PET and PVA gel which utilises KCl and $Zn(CH_3COO)_2$ in deionized water as an electrolyte. The performance of this flexible ECB is shown in Table 1, demonstrating the capacity of the Zn/PPY ECB is higher than that of reported aqueous electrolyte based ESC [85]. The electrochromic property of this battery shows that at 1.2 V the battery display turns black in colour and the black colour lightens when it is discharged to 0.8 V. Finally at a voltage of 0.4 V the Zn//PPy battery became dark yellow. Further studies of this material under different bending conditions, the bleaching and colouring time, and colouration efficiency need to be investigated [85].

4.4. Separators and protective/insulative materials used in EESDs

Flexibility and transparency are key factors in the fabrication of flexible EESDs. To date the majority of flexible EESD fabrication used hydrogel electrolytes which function as both separator and electrolyte [51,53,85,128] due to the presence of both polymers and salts. A detailed discussion of various electrolytes used for EESD fabrication was given in section 4.2. In one report, using a CNTs/Au/PPy/PET based electrode a 1 mm thick PDMS frame was used as a separator and in which the $LiClO_4$ aqueous electrolyte was injected [129]. In a wire-shaped ECB, the SPANI@Au/nylon 66 functions as a cathodic electrode and a separator [130]. For another ECB, $AlCl_3$ was coated on an AGM as the electrolyte/separator and in which the AGM exhibited high wettability (details provided in section 3.2.). In addition to the electrolyte/separator, in the fabrication of flexible ESCs and ECBs, ITO, PET or other insulative polymers were used as the substrate. These substrates will also be used as a protective layer for the flexible EESD. In some devices, double faced adhesive

tape was used to separate the active electrodes [131] and an epoxy sealant was used as an encapsulation materials [33]. To further enhance the life cycle of the flexible EESD and to provide protection from the environment, further studies are required with regard to separators and encapsulation materials.

5. Fabrication technology: Large area flexible EESD

Studies on various devices show that along with material selection, the fabrication methods employed have a significant influence on the performance of devices. There are various fabrication methods, including ink jet printing, spin coating, electrodeposition and electrostatic spray deposition (ESD) employed for the electrodes design [33]. When considering the practical implementation of EESDs, fabrication methods for both large and small area devices, dependent upon specific application, must be developed. For large area electrodes (e.g. 1 m x 1 m), the film deposition methods are critical. Among these methods, ESDs based on electrostatic interaction mechanisms show significant advantages including (i) being simple and cost-effective, (ii) enable direct deposition on cc/substrate without any binder/additives (iii) use an ambient atmosphere without any high vacuum or temperature and (iv) provide efficient utilisation of materials [33]. The ESD shown in Fig. 14**a** consists of three major parts including high-DC voltage supply, a syringe connected with a metal nozzle, and a conductive substrate. By utilising this method presented in Fig. 14b, a bendable and rollable Fe (II)-based metallo-supramolecular polymer (polyFe) film based ECB device (27 × 30 cm^2) was developed on an ITO/PET substrates. Here, the polyFe film shows excellent performance for electrochromic energy efficient applications such as large modulation (73.6 %), fast switching speed (T_b- 1.7 s and T_c- 1.4 s.), ultrahigh colouration efficiency (717.2 cm^2. C^{-1} for flexible EESD), robust stability (up to 10,000 cycles even on flexible substrate) and high gravimetric capacity (18.24 mA. h. g^{-1} at current densities of 0.75 A. g^{-1}) [33]. The authors observed that the obtained gravimetric energy density is less than that of MO_x or polymer based EESDs.

A distinctive feature of this work is the development of a simple, large area manufacturing process, with further modification of the material leading to future performance enhancement. In addition, a smart energy storage indicator cue is provided by the polyFe electrode. Furthermore, the authors also developed polyFe and TiO_2 film based flexible EESDs with a $LiClO_4$/PMMA-based electrolyte as presented in Fig. 14c, showing a CE of 728.7 cm^2. C^{-1} and large optical modulation (55 % at 581 nm, with fast switching speed of T_b – 0.8 and T_c 0.6 s) [33].

In flexible electronics technology, roll-to-roll (R2R) printing [134] has been highly successful in the fabrication of large area electrodes (hundreds of meters per minute) on polymer/plastic/paper substrates, with low cost and high throughput [135]. The major advantage of this method is the ability for hybrid integration of organic and inorganic components [135]. This R2R method has been successfully demonstrated for the development of electrochromic windows through the deposition of Ag nanofiber networks on PET

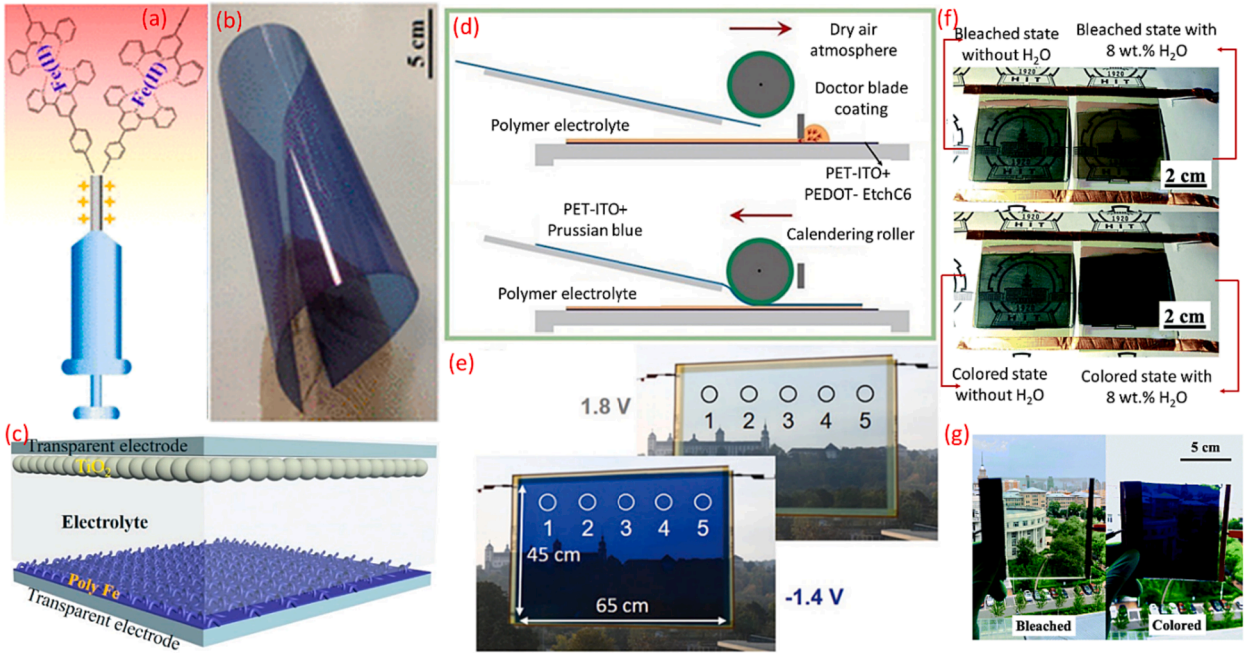

Fig. 14. (a) Schematic of electrostatic spray deposition strategy to fabricate high-quality polyFe electrochromic film. (b) Flexible polyFe electrochromic film. (c) The polyFe electrochromic based flexible EESD with $LiClO_4$/PMMA-gel electrolyte. (a-c) Reprinted (adapted) with permission from [33] Copyright (2020) American Chemical Society. (d) Schematic representation of fabrication of large area flexible EESD using PEDOT-EthC6/PB by roll-to-roll printing method [132] and (e) and photographic images large area PEDOT-EthC6/PB based EESD window in coloured and bleached stage [132]. (f) Photos of flexible ITO/WO_3/electrolyte/NiO/ITO assembled EESD (16 cm^2) using a non-aqueous electrolyte (top) and the electrolyte with 8 wt% of H_2O (bottom) (g) EESD ITO/WO_3/electrolyte/NiO/ITO assembled EESD in glass substrate with electrolyte with 8 wt% of H_2O at 1.4 V. (f-g) Reprinted (adapted) with permission from [133]Copyright (2012) Royal Society of Chemistry.

substrates as given inn Fig. 14d, realising an electrical resistance of 12Ωsq^{-1} and transmittance of 95 % [136]. By using this method a large area of 45 x 65 cm^2 (Fig. 14e) has been demonstrated with the possibility of fabrication of 50 cm active width and 100 cm active length smart windows[132]. For such large area electrodes, fabrication of two types of electrode such as poly(3,4-ethylene dioxythiophene) (PEDOT) derivative (PEDOT-EthC6) and Prussian blue (PB) were used. In which PEDOT-EthC6 acts as cathodic colouring and PB functions as the anodic colouring material. The fabricated flexible EESDs could be potentiostatically switched between − 1.4 and 1.8 V dark and bleached states respectively[132]. The reported CE value of this device is 563 cm^2. C^{-1}, much higher than other reported PEDOT:PSS based electrochromic devices [132]. A further investigation on energy storing performance of this device in static and dynamic bending will enrich the research analysis of this work. For an industrial large area application, electrode fabrication via electron beam evaporation has also been found to be a promising method [133]. A flexible ITO/WO_3/electrolyte/NiO/ITO assembled EESD with anion-assisted electrochromism shows the possibility of large area EESD fabrication. As proof of concept, a 4 x 4 cm^2 flexible substrate and 10 x 10 cm^2 ITO/Glass substrate device was developed as shown in Fig. 14f and 14 g [133]. A flexible EESD with 16 cm^2 area in 8 wt% of H_2O exhibits an obvious contrast between the coloured and bleached states as compared with an electrolyte without H_2O [133].

In electrochemical energy storage device fabrication, MXenes (carbonitrides), have received significant interest due to their excellent electronic and stable electrochemical properties [137–139]. Such 2D materials are robust against environmental factors including high temperature and mechanical wear. Due to these properties, in addition to its unique optical and electrical parameters MXene could be potentially used for future EESD fabrication. MXene is also widely reported as a template for the synthesis of nanostructured transition metal oxides (TMO) [140,141]. In one of these reports, self-assembled MXene/TMO heterostructure materials show flexible transparent conductive electrodes and the TMO that is derived from MXene exhibits electrochromic properties [142]. Recently, 2D material structures (e.g., MXene) and their derivative TMOs have found application for large area flexible EESD fabrication. Large area flexible electrodes for EESDs have been fabricated by a liquid/liquid interfacial self-assembly (LLIA) technique using homogeneous thin films of the TiO_2 or $Ti_3C_2T_x$ network [142]. The layered electrode assembly employed is shown in Fig. 15**a**. As discussed previously, these MXene/TMO heterostructures also show excellent electrochromic performance and uniform colour distribution in their bent state (proved for 3 mm and 1.5 cm bending radius). The attractive performance of these flexible EESD materials is due to the loosely networked structure of the TiO_2 in which the Li ion transportation occurs via two methods: (i) ions enter through the top surface and (ii) ions travel through all individual nanostructures of the materials as shown in Fig. 15b [142]. As compared to dense films, the second ion pathway is dominant in loosely structured nanomaterials and hence shows excellent CE for the EESD. Fig. 15c displays an A4 size (20 x 30 cm) flexible EESD which maintains its colouration state after disconnection from the voltage supply [142].

Along with large area, possible bending angle is also critical for flexible EESDs [143]. In one report, a multi MO_x layer was deposited on a PET substrate by using magnetron sputtering. It was found that solid-state monolithic coatings ITO/WO_3/Nb_2O_5/$NiVO_\chi$/ITO as given in Fig. 16**a** of the materials on flexible polymers show excellent performance in different bending radii and the device could be realised with an effective area of 24 cm × 18 cm [143]. Fig. 16b presents the transmittance spectra of the EESD under colouring and bleaching states for different bending radii. Furthermore, it was noted that the response time for colouring and bleaching is not influenced by different bending radii, as shown in Fig. 16c and 16d. The analysis predicts that the device could operate up to 7.5 cm bending radius and beyond this bend radius the film would start to crack, affecting the device performances [143].

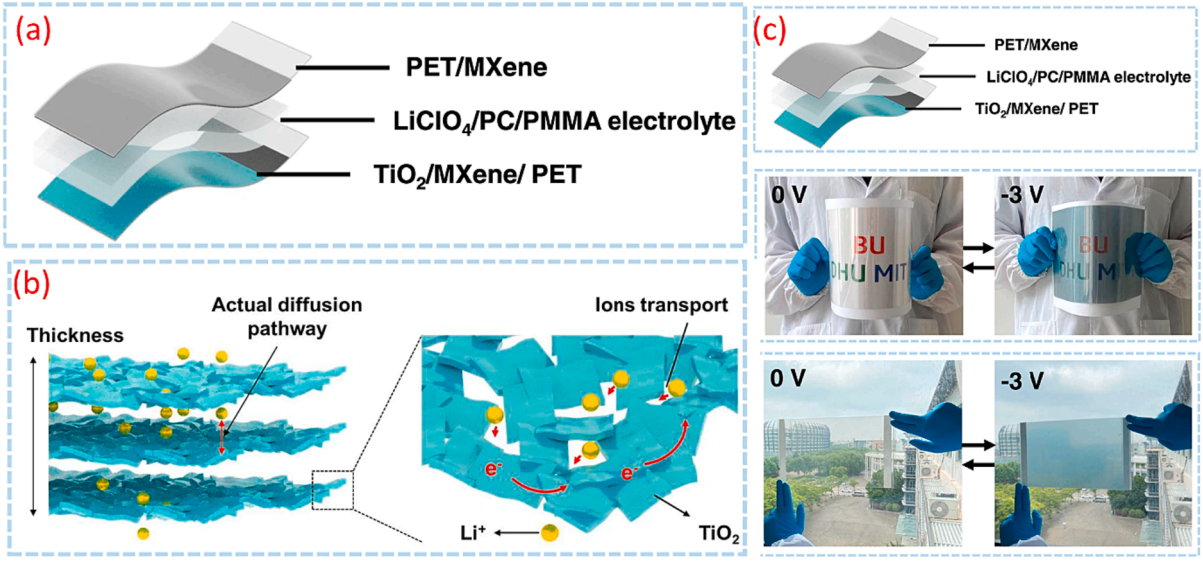

Fig. 15. (a) Schematic representation of Mxene based flexible EESD [142]. (b) Schematic representation of the pathways of electron conduction and ion diffusion from electrolyte within the self-assembled TiO_2 thin film [142] (c) Image of large area flexible Mxene based EESD in different oxidation state [142].

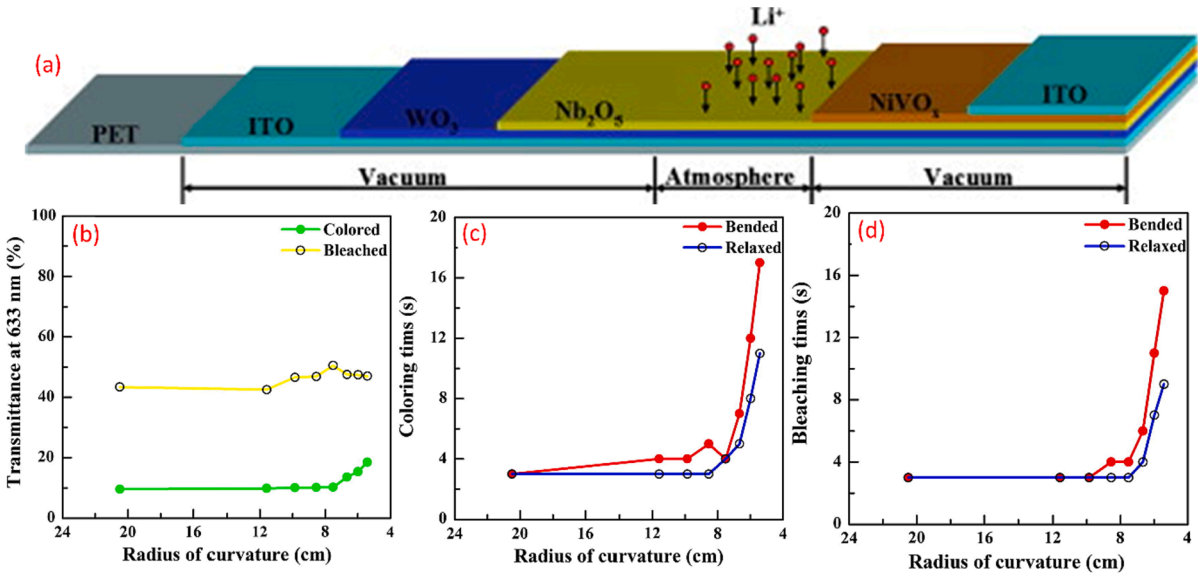

Fig. 16. (a) Layered monolithic structure of the flexible EESD constructed based on ITO/WO_3/Nb_2O_5/$NiVO_\chi$/ITO [143] and its (b) transmittance, (c) colouring time and (d) bleaching time for of the 3.5 cm × 5.5 cm EESD under different radii of curvature in static bending. Reprinted from [143] Copyright (2016), with permission from Elsevier.

6. Applications and need for flexible and stretchable EESDs

The advantages of both electrochromic and electrochemical energy storage make the EESD a strong candidate for implementation in advanced energy system for emerging applications. The significance of flexible and conformable energy sources with high-energy storage capability, and fast charging-discharging rates are essential for e.g., smart wearables, robots, electric vehicles, etc. The multiple functionalities of EESDs lead to their potential implementation in various applications including integration with smart windows of building, aircrafts windows, robots, electric vehicles, wearable electronics, healthcare monitoring devices, colour-changing sunglasses, heads-up displays, etc.. One of the unique properties of an EESD is its function as an indicator of energy storage level, providing a visual cue through transparency and/or colour changes. In many reports, the practical application of flexible EESDs, has been demonstrated by operating an LED. One example is given in Fig. 17**a** in which a flexible EESD, based on amorphous-quantized $WO_3{\cdot}H_2O$, powered an LED [52]. The practical application of EESDs manufactured form different materials may be determined by the different voltage levels and/or colours of the device. For example for flexible ECBs, the transmittance may change from orange to yellow at different voltage levels [85]. Similarly, it was noted that this flexible ECB exhibited a short circuit chromatic warning function. In a normal electric circuit, the flexible ECB was black whilst powering a clock. However, in a short circuit condition, the ECB immediately turned bright yellow and the clock turned off [85]. These colour variation and energy storage capacity can be implemented for smart window and wearable applications.

6.1. *EESD as a smart window*

In a smart building, heat exchange and light emission may be controlled by using electrochromic windows [144–147]. Such electrochromic layers for controlling heat and light exchange have significant advantages in net zero emission and decarbonisation [38,88,148,149]. For example, recent studies show that the annual energy consumption of buildings is ~ 40 % of the world's total energy consumption and among this the major portion is expended in doors and windows [150,151]. This is due to limitations of controlling heat exchange and light transmission between the indoor and outdoor environment. EESD integration with windows would allow the control of the light intensity during charging/discharging. However, the CE is strongly influenced by the charge density of the EESD. A controlled charge delivery (charge insertion or extraction) will define the transmittance of the window for light and heat which is termed as bright mode, cool mode, and dark mode as shown in Fig. 18. A schematic representation of this mechanism and the smart window concept is described in Fig. 18.

As an example, in the case of smart glass, when the storage cell is fully charged, at open circuit voltage, the electrochromic window is in bright mode and its colour is dependent on the type of material used. In this mode, both heat and natural light enter through the glass. During discharging, if the voltage is halved, the window will be in cool mode. In cool mode, the window blocks the transmission of heat and allows the transmission of light [53]. When the EESD is at a lower voltage (less than half), the window will be in dark mode. In dark mode the EESD window limits the flow of heat and light. Such windows have significant advantages in minimizing light pollution and in reducing energy consumption in buildings. In addition to the feature of electrochromicity, the energy stored in the window could be used as an energy source for powering sensors including humidity, temperature, and gas (CO_2, NO_x) monitoring

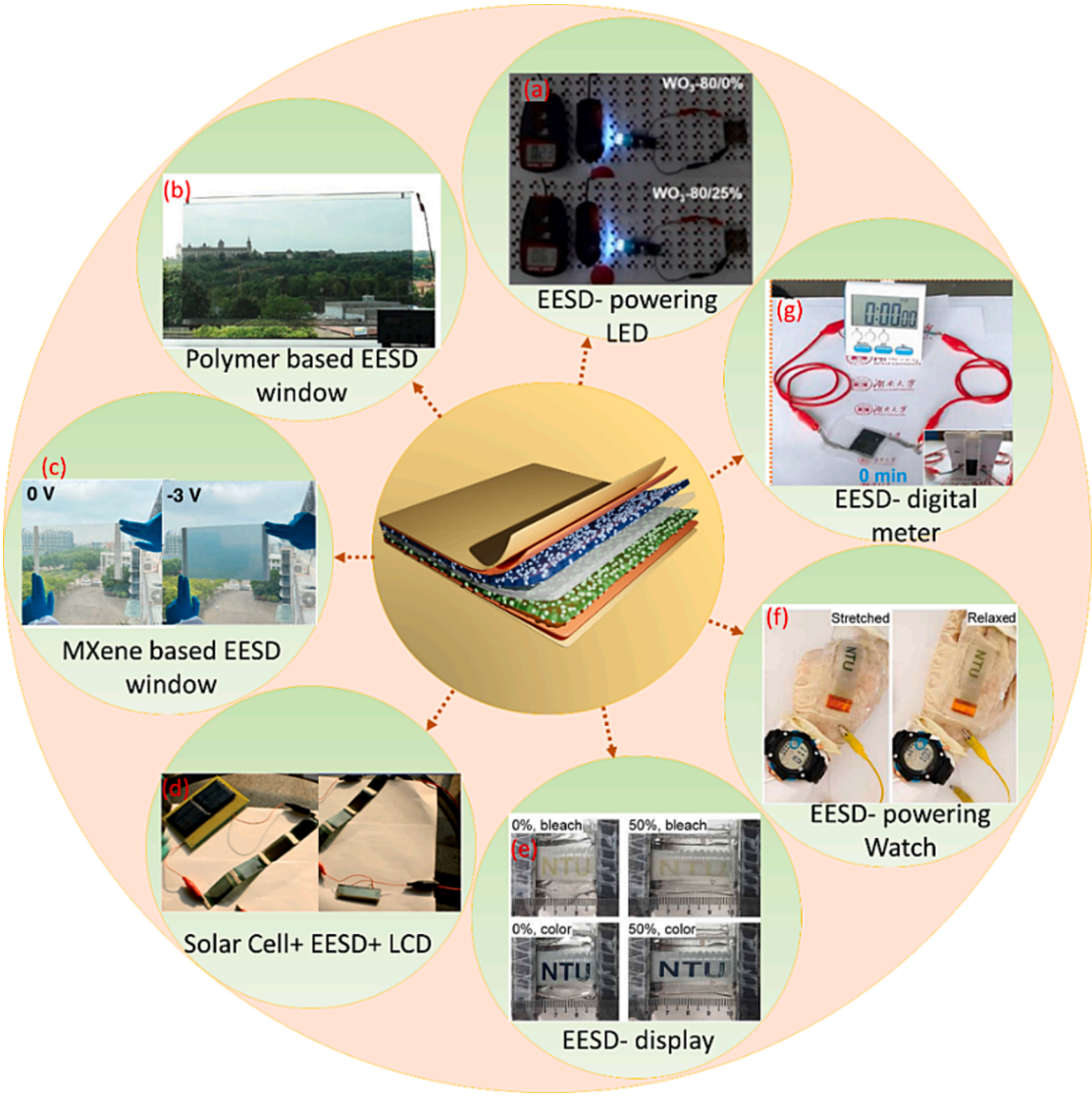

Fig. 17. Application of flexible and stretchable EESD (a) demonstration of WO_3 based EESD for lighting a LED [52] Reprinted from Publication [52] Copyright (2021), with permission from Elsevier. (b) PEDOT-EthC6/PB based large area flexible window [132] (c) large area MXene based window in different potential [142]. (d) Integration of solar cell with EESD for powering LCD and its implementation for self-powered system [123] (e) and (f) flexible EESD shows its function as display and integrated for powering smart watch [152]. (g) powering hybrid bimetal hydroxide based EESD for a digital meter. Reprinted (adapted) with permission from [96] Copyright (2021) John Wiley and Sons.

(either during night or during bright or cool mode) which may be used for building health monitoring. Multiple integration of such EESDs (increasing capacity or potential) with advanced energy distribution, following grid concepts and power management, allows the stored energy to be used for powering other devices in the home or workplace (e.g., light, building alarm). For smart window applications, area scalable manufacturing is required. The oxidation and reduction reactions at different voltage could control the transparency or coloured state of the window. Fig. 17b and 17c denotes the implementation of MXene [142] and PEDOT-EthC6/PB [132] based flexible EESD in large area smart windows.

6.2. *Integration of renewable power sources with EESDs*

The charging of EESDs using external (wired) power sources has practical limitations, but this could be overcome by integration with solar cells. A very promising application of combined EESD/solar cell devices is as a smart window, replacing the glazed glass to control both light and heat [123]. To demonstrate this application, PANI NW based flexible ESCs were integrated with a solar cell to function as an energy storage smart window (ESS window) [123]. Fig. 17d shows the image of the ESS window and its application to power an LCD. Another study shows that based on the intensity of the incident light, the colouration of the EESD was controlled and

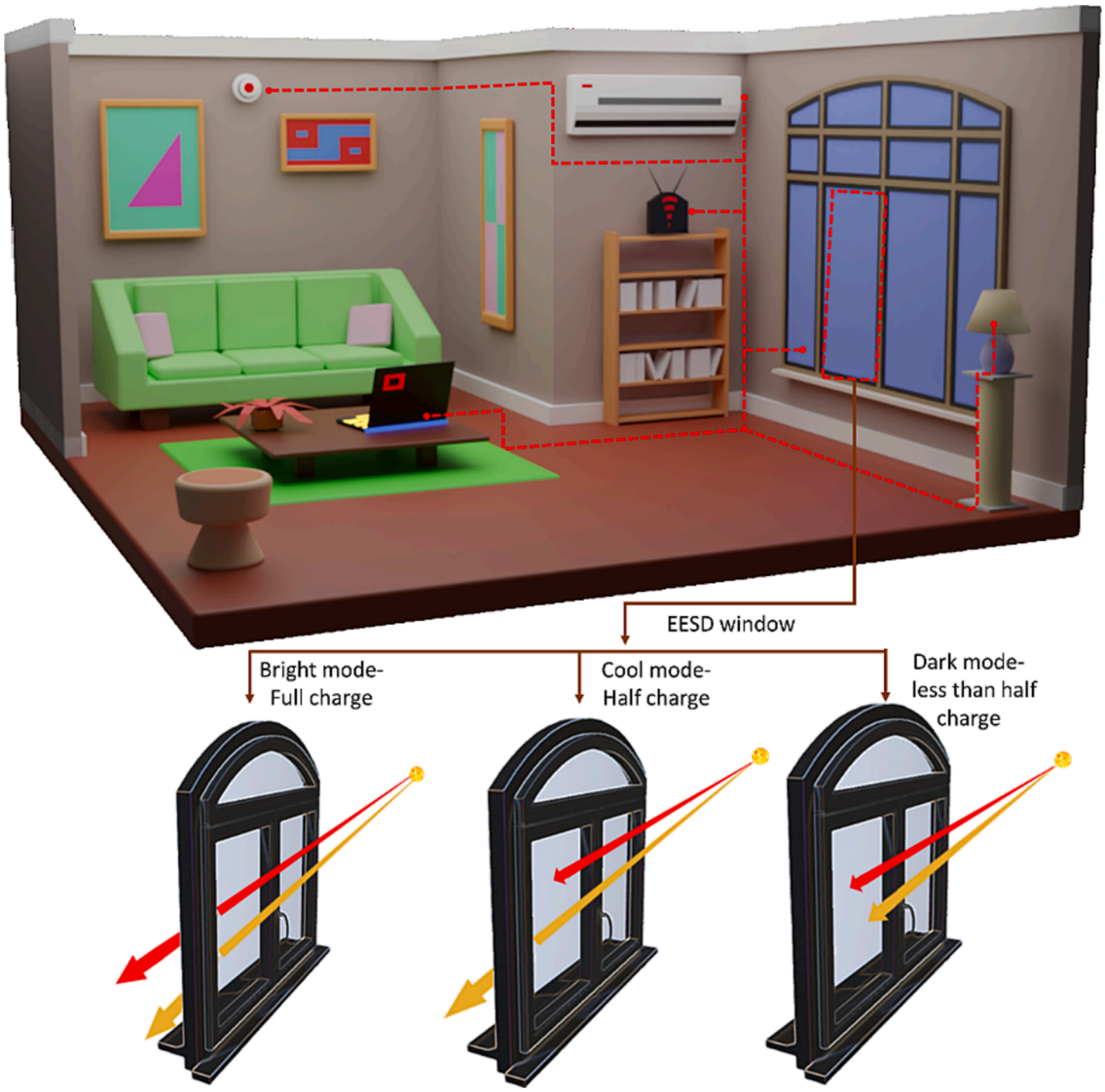

Fig. 18. Energy distribution in powering different devices in room (alarm sensors, portable components, controlling heat and light) by EESD in day and nighttime using different charging conditions.

such device could be act as autonomous device for self-powered applications [53]. In addition to this, a solar driven flexible electrochromic SC, in which the EESD is integrated with dye-sensitized solar cells (DSSC) has also been developed [54]. This work utilised integrated DSSCs and EESDs in a single module rather than through connection to a photovoltaic (PV) cell through a wired connection. The DSSC consists of DSSC ITO-PET electrode, electrolyte, TiO_2 film and the Pt electrode. The EESD consists of ITO-PET electrode, electrolyte, WO_3 film and the Pt electrode. Both the DSSC and EESD share an ITO-PET electrode, electrolyte and the Pt electrode. Considering the future concept of low energy green buildings, the photochromism mechanism (convert solar energy by DSSC into electricity to charge the EESD) may allow the achievement of zero energy consumption [54].

6.3. EESD for wearable system and low power electronics

For a wearable system, flexible and stretchable EESDs could be potentially used as an indicator of energy storage, and the energy sources for powering transparent displays, sensors, human–machine interfaces and other IoT devices [37,88,152,153]. In wearable systems, different sensors (physical, chemical, biological parameters monitoring) require different ranges of power depending on the sensor type and its design [154–157]. In addition to the sensors, related components (electronics for data acquisition, analysis and communication) require different power ranges as shown in Fig. 19. Accordingly, there are different energy generators and storage systems reported for wearable applications [156–159]. Among these, the major advantage of the EESD is its dual functionality, electrochromic property and energy storage [47,160,161]. These advantages make EESDs appealing for health monitoring sensors,

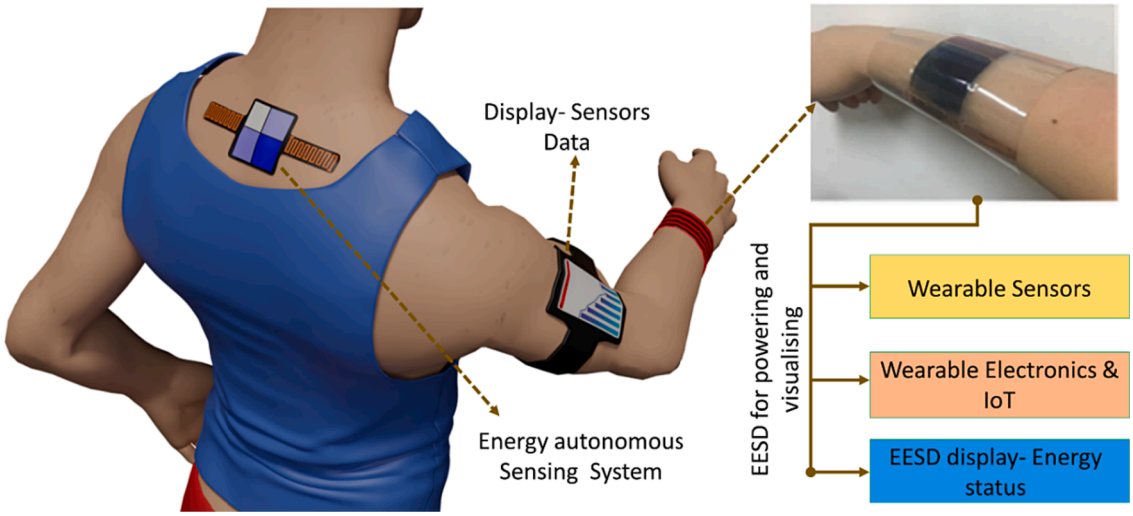

Fig. 19. The potential implementation of EESD in wearable applications. The image for hand with EESD obtained from [54].

sports sensors, and fashion.

A stretchable EESD using inkjet-printing of WO_3 nanoparticles has been developed which exhibited excellent electrochromic (CE- 75.5 cm^2. C^{-1}, switching speed < 4.5 s, optical modulation 40 %) and electrochemical performances (specific capacity- 32.3 mA. h. g^{-1}) [152]. Persistent colouring-bleaching (1000 s, 250 switching cycle), and cyclic bending (strain 50 %) shows that the device performs similarly to the initial performances. The specific capacity and mechanical stability of the device is attractive for application in wearable system and the authors demonstrated a display application as shown in Fig. 17e and 17f [152]. The high performance and mechanical flexibility of hybrid flexible EESDs using bimetallic hydroxide (NiCO-BH) has found potential implementation in powering digital meters, as shown in Fig. 17g and wearable devices (powering a watch) [96]. The performance of stretchable EESDs were also demonstrated for wearable systems by attaching devices on the wrist. The reversible coloured (−1.5 V) into bleached state (−0.1 V) and stable operation under cyclic stretching (20 % strain) underlines suitability for applications in powering wearable electronics [37].

7. Future perspective and summary

With the focus on the net zero target [162,163] and significant development in wearable and portable electronic devices, research in new energy storage devices is highly propitious. The distinct properties of EESDs as compared to other SCs and batteries, and emerging studies on flexible and stretchable EESDs will be attractive for developing future sustainable energy systems. The development and application of inorganic materials such as metal oxide coatings (requiring high temperature deposition processes) may pave the way to achieve high performance films. However, polymeric or plastic substrates have difficulties in withstanding high processing temperatures. This issue could be overcome using ultra-thin transparent film coated glasses. Such films exhibit high transparency and low sheet resistance. For example, recently a flexible EESD fabricated using ultra-thin ITO coated glass (100 μm thickness) demonstrated 88 % transmittance, and a sheet resistance of 23 Ω. sq^{-1} [164]. In a rigid EESD, it was observed that the high density of oxygen vacancies associated with nonstoichiometric $W_{18}O_{49}$ nanowires (WNS) realises an excellent electrochromic cathodic material. However, one of the drawbacks of WNS is its reduction in the outer contact area due to its ease in aggregation into large structures during manufacture. This issue could be overcome by chemically treating with rGO which contains a large number of oxygen-containing functional groups [72]. While reacting with WNS, it strongly couples to form a new composite material rGO-WNS, enhancing ion diffusion. The electrochemical and electrochromic properties of WNS and rGO-WNS [72] indicate that rGO-WNS has better performance for electrochromic applications. The reduction in optical modulation could be due to the obstruction of graphene to light transmittance. rGO-WNS based cathodic ECMs show excellent performance with the combination of anodic PANI films. PANI shows a rich colour change from light green to green to dark blue during electrochromic reaction [72]. It was noted that for a full cell of rGO-WNS and PANI in H_2SO_4 electrolyte, the colour change of PANI film during the electrochemical reaction was light green -dark green – light blue - dark blue, as shown in Fig. 3c [72]. Further studies of this film using stretchable and flexible substrates under different (cyclical) bending angles, along with the investigation of long-term stability (evaporation of electrolyte) will be beneficial for flexible EESD.

Additionally, fully screen printed thin film active-matrix electrochromic displays have been demonstrated [165]. This device comprises silver (Ag) nanoparticles, semiconducting single-wall carbon nanotubes (SWCNTs), and barium titanate (BTO) as the conductor, conduction channel, and an insulator on a PET substrate [165]. The Ag/electrolyte/PEDOT:PSS lateral architecture was fabricated for active-matrix electrochromic display characterisation with PEDOT:PSS acting as the active material for colouration. They reported an on-state current density of 3.62 μA. mm^{-1} at a gate voltage (V_G) = -15 V when the SWCNT TFT was at a source drain voltage (V_{DS}) = -1 V, as well as an average on–off ratio of 10^4. Furthermore, excellent electrical performance with an average mobility

of 3.92 ± 1.08 cm^2. V^{-1}. S^{-1} was obtained for a fully printed backplane. The electrochromic cell exhibited a switching time of 2 ~ 5 s, which was in good agreement with a lateral electrochromic cell already reported [165]. It was observed that the voltage-current characteristics of the printed electrochromic cell operates reliably under bending radii of 5, 10, 15 and 20 cm, and in the relaxed state. The changes in applied bias from −3 to 3 V leads to a maximum current flow of 25 μA, however, upon applying ~ 5 V the PEDOT: PSS oxidized with exponentially dropped in current from 25 μA to 13 μA. The electrochromic cell switching characteristics bias between −3 V and 3 V, and the back to −3 V for 5 to 100 cycles exhibiting excellent cyclability and outstanding non-degradation of the electrical performance after a week.

These characteristics suggest that fully screen-printed lateral structure electrochromic cells, fabricated on flexible substrate, have outstanding stability in the ambient environment, excellent electrical performance, and remarkable cyclability. Such screen printed EESDs will have advantages for large area fabrication for smart windows. In addition, to enhance the electrochromic and energy storing performance, hybrid material composite based ESCs and ECBs will be advantageous, along with multivalent cation-based gel electrolytes. Initial electrochromic and electrochemical studies on pulser laser deposited metal oxide nanostructured film have shown remarkable optical and structural properties [166–168] and require further development and investigation. The energy control of EESDs is critical and a new hierarchical layout optimisation method is required for large scale integration of renewable energy sources (e.g., solar cell) maximising energy balance and minimising loss [169,170].

In summary, we have provided a detailed review of the various electrochromic energy storage materials' structural, morphological, elemental, electrical, electrochromic, optical and electrochemical properties. The inclusion of various materials in this review shows that various transparent and electrochromic materials have significant advantages for the development of flexible and stretchable electrochromic energy storage devices. Such flexible and stretchable electrochromic energy storage devices have multiple functionalities and could be potentially implemented for wearables, smart building, electric vehicles, and smart display. A controlled power management circuit design for charging and discharging will enable the electrochromic energy storage for controlling the light/display and energy. Previous studies on ESCs and ECBs reveal significant progress and future promise, and that continued performance improvement of the devices through the use of different materials, hybrid approaches, and the development of fabrication technologies will lead to practical applications.

CRediT authorship contribution statement

Libu Manjakkal: . **Luis Pereira:** Conceptualization, Funding acquisition, Investigation, Methodology, Writing – original draft, Writing – review & editing. **Eric Kumi Barimah:** . **Paul Grey:** Investigation, Visualization, Writing – original draft. **Fabiane F. Franco:** Investigation, Visualization, Writing – original draft. **Zhengyu Lin:** Investigation, Writing – original draft. **Gin Jose:** Funding acquisition, Investigation, Methodology, Writing – original draft. **Richard A. Hogg:** Conceptualization, Writing – original draft, Writing – review & editing.

Declaration of Competing Interest

The authors declare that they have no known competing financial interests or personal relationships that could have appeared to influence the work reported in this paper.

Data availability

Data will be made available on request.

Acknowledgements

This work is supported by the Edinburgh Napier University SCEBE Starter Grant (N480-000). This work was supported by the European Commission through the AQUASENSE (H2020-MSCA-ITN-2018-813680) project and NERC discipline hopping activities to tackle environmental challenges project (SEED-2022-317475). This work was also supported by the FEDER funds through the COMPETE 2020 Program and the National Funds through the FCT – Portuguese Foundation for Science and Technology under Project No. POCI-01-0145-FEDER-007688,(UID/CTM/50025), project CELLECTIVE,(PTDC/CTM-CTM/4653/2021) and project SMART-E, (2022.04012.PTDC). PG acknowledges the support from the FCT – Fundação para a Ciência e a Tecnologia, I.P. through scholarship PTDC/NAN-MAT/32558/2017. LP acknowledged the European Commission under project SYNERGY (H2020-WIDESPREAD-2020-5, CSA, GA 952169), and project EMERGE (H2020 -INFRAIA-2020-1, GA 101008701). GJ acknowledged EPSRC grant (EP/T004711/1).

References

[1] Ruhnau O, Bannik S, Otten S, Praktiknjo A, Robinius M. Direct or indirect electrification? A review of heat generation and road transport decarbonisation scenarios for Germany 2050. Energy 2019;166:989–99.
[2] Kannan R. Uncertainties in key low carbon power generation technologies–Implication for UK decarbonisation targets. Appl Energ 2009;86(10):1873–86.
[3] Di Silvestre ML, Favuzza S, Sanseverino ER, Zizzo G. How Decarbonization, Digitalization and Decentralization are changing key power infrastructures. Renew Sust Energ Rev 2018;93:483–98.

[4] Arabzadeh V, Mikkola J, Jasiūnas J, Lund PD. Deep decarbonization of urban energy systems through renewable energy and sector-coupling flexibility strategies. J Environ Manage 2020;260:110090.
[5] Bloess A, Schill W-P, Zerrahn A. Power-to-heat for renewable energy integration: A review of technologies, modeling approaches, and flexibility potentials. Appl Energ 2018;212:1611–26.
[6] Gielen D, Boshell F, Saygin D, Bazilian MD, Wagner N, Gorini R. The role of renewable energy in the global energy transformation, Energy. Strateg Rev 2019; 24:38–50.
[7] Hannan M, Faisal M, Ker PJ, Begum R, Dong Z, Zhang C. Review of optimal methods and algorithms for sizing energy storage systems to achieve decarbonization in microgrid applications. Renew Sust Energ Rev 2020;131:110022.
[8] Rangel-Martinez D, Nigam K, Ricardez-Sandoval LA. Machine learning on sustainable energy: A review and outlook on renewable energy systems, catalysis, smart grid and energy storage. Chem Eng Res Des 2021;174:414–41.
[9] Luo J, Hu B, Hu M, Zhao Y, Liu TL. Status and prospects of organic redox flow batteries toward sustainable energy storage. ACS Energ Lett 2019;4(9):2220–40.
[10] Alami AH. Mechanical energy storage for renewable and sustainable energy resources. Springer; 2020.
[11] Aşchilean I, Cobîrzan N, Bolboaca A, Boieru R, Felseghi RA. Pairing solar power to sustainable energy storage solutions within a residential building: A case study. Int J Energ Res 2021;45(10):15495–511.
[12] Dong P, Rodrigues M-T-F, Zhang J, Borges RS, Kalaga K, Reddy AL, et al. A flexible solar cell/supercapacitor integrated energy device. Nano Energy 2017;42: 181–6.
[13] Gurung A, Qiao Q. Solar charging batteries: advances, challenges, and opportunities. Joule 2018;2(7):1217–30.
[14] Zahedi A. Maximizing solar PV energy penetration using energy storage technology. Renew Sust Energ Rev 2011;15(1):866–70.
[15] Kato N, Higuchi K, Tanaka H, Nakajima J, Sano T, Toyoda T. Improvement in long-term stability of dye-sensitized solar cell for outdoor use. Solar Energ Mater Sol 2011;C.95(1):301–5.
[16] Manjakkal L, Núñez CG, Dang W, Dahiya R. Flexible self-charging supercapacitor based on graphene-Ag-3D graphene foam electrodes. Nano Energy 2018;51: 604–12. self-reference.
[17] Manjakkal L, Pullanchiyodan A, Yogeswaran N, Hosseini ES, Dahiya R. A Wearable Supercapacitor Based on Conductive PEDOT:PSS-Coated Cloth and a Sweat Electrolyte. Adv Mater 2020;32(24):1907254. self-reference.
[18] Manjakkal L, Navaraj WT, Núñez CG, Dahiya R. Graphene-Graphite Polyurethane Composite Based High-Energy Density Flexible Supercapacitors. Adv Sci 2019;6(7):1802251. self-reference.
[19] Phan D, Bab-Hadiashar A, Lai CY, Crawford B, Hoseinnezhad R, Jazar RN, et al. Intelligent energy management system for conventional autonomous vehicles. Energy 2020;191:116476.
[20] Karden E, Ploumen S, Fricke B, Miller T, Snyder K. Energy storage devices for future hybrid electric vehicles. J Power Sources 2007;168(1):2–11.
[21] Kouchachvili L, Yaïci W, Entchev E. Hybrid battery/supercapacitor energy storage system for the electric vehicles. J Power Sources 2018;374:237–48.
[22] Boukoberine MN, Zhou Z, Benbouzid M. Power supply architectures for drones-a review, IECON 2019–45th Annual Conference of the IEEE Industrial Electronics Society. IEEE 2019:5826–31.
[23] Pullanchiyodan A, Manjakkal L, Ntagios M, Dahiya R. MnOx-Electrodeposited Fabric-Based Stretchable Supercapacitors with Intrinsic Strain Sensing. ACS Appl Mater Inter 2021;13(40):47581–92. self-reference.
[24] Khaligh A, Li Z. Battery, ultracapacitor, fuel cell, and hybrid energy storage systems for electric, hybrid electric, fuel cell, and plug-in hybrid electric vehicles: State of the art. IEEE T Veh Technol 2010;59(6):2806–14.
[25] García Núñez C, Manjakkal L, Dahiya R. Energy autonomous electronic skin, npj Flexible Electron 2019;3(1):1. self-reference.
[26] Santos L, Wojcik P, Pinto JV, Elangovan E, Viegas J, Pereira L, et al. Electrochemical Devices: Structure and Morphologic Influence of WO3 Nanoparticles on the Electrochromic Performance of Dual-Phase a-WO3/WO3 Inkjet Printed Films. Adv Electron Mater 2015;1(1–2):1400002. self-reference.
[27] Wojcik PJ, Santos L, Pereira L, Martins R, Fortunato E. Tailoring nanoscale properties of tungsten oxide for inkjet printed electrochromic devices. Nanoscale 2015;7(5):1696–708. self-reference.
[28] Yang P, Sun P, Mai W. Electrochromic energy storage devices. Mater today 2016;19(7):394–402.
[29] Wang H, Yao C-J, Nie H-J, Yang L, Mei S, Zhang Q. Recent progress in integrated functional electrochromic energy storage devices. J Mater Chem C 2020;8 (44):15507–25.
[30] Liu L, Du K, He Z, Wang T, Zhong X, Ma T, et al. High-temperature adaptive and robust ultra-thin inorganic all-solid-state smart electrochromic energy storage devices. Nano Energy 2019;62:46–54.
[31] Wang L, Guo M, Zhan J, Jiao X, Chen D, Wang T. A new design of an electrochromic energy storage device with high capacity, long cycle lifetime and multicolor display. J Mater Chem A 2020;8(33):17098–105.
[32] Laschuk NO, Ebralidze II, Easton EB, Zenkina OV. Systematic Design of Electrochromic Energy Storage Devices Based on Metal-Organic Monolayers. ACS Appl Energ Mater 2021;4(4):3469–79.
[33] Cai G, Chen J, Xiong J, Lee-Sie Eh A, Wang J, Higuchi M, et al. Molecular Level Assembly for High-Performance Flexible Electrochromic Energy-Storage Devices. ACS Energ Lett 2020;5(4):1159–66.
[34] Pathak DK, Moon HC. Recent progress in electrochromic energy storage materials and devices: a minireview. Mater Horiz 2022;9(12):2949–75.
[35] Xia X, Ku Z, Zhou D, Zhong Y, Zhang Y, Wang Y, et al. Perovskite solar cell powered electrochromic batteries for smart windows. Mater Horiz 2016;3(6): 588–95.
[36] Zhang J, Yang J, Leftheriotis G, Huang H, Xia Y, Liang C, et al. Integrated photo-chargeable electrochromic energy-storage devices. Electrochim Acta 2020; 345:136235.
[37] Yun TG, Park M, Kim D-H, Kim D, Cheong JY, Bae JG, et al. All-transparent stretchable electrochromic supercapacitor wearable patch device. ACS Nano 2019; 13(3):3141–50.
[38] Korgel BA. Composite for smarter windows. Nature 2013;500(7462):278–9.
[39] Österholm AM, Shen DE, Kerszulis JA, Bulloch RH, Kuepfert M, Dyer AL, et al. Four Shades of Brown: Tuning of Electrochromic Polymer Blends Toward High-Contrast Eyewear. ACS Appl Mater Inter 2015;7(3):1413–21.
[40] Bi Z, Li X, Chen Y, He X, Xu X, Gao X. Large-Scale Multifunctional Electrochromic-Energy Storage Device Based on Tungsten Trioxide Monohydrate Nanosheets and Prussian White. ACS Appl Mater Inter 2017;9(35):29872–80.
[41] Xue J, Xu H, Wang S, Hao T, Yang Y, Zhang X, et al. Design and synthesis of 2D rGO/NiO heterostructure composites for high-performance electrochromic energy storage. Appl Surf Sci 2021;565:150512.
[42] Wang W-Q, Wang X-L, Xia X-H, Yao Z-J, Zhong Y, Tu J-P. Enhanced electrochromic and energy storage performance in mesoporous WO_3 film and its application in a bi-functional smart window. Nanoscale 2018;10(17):8162–9.
[43] Bi Z, Li X, He X, Chen Y, Xu X, Gao X. Integrated electrochromism and energy storage applications based on tungsten trioxide monohydrate nanosheets by novel one-step low temperature synthesis, Solar Energ. Mater. Solar Cells 2018;183:59–65.
[44] Wang J, Huo X, Guo M, Zhang M. A review of NiO-based electrochromic-energy storage bifunctional material and integrated device. J Energy Storage 2021: 103597.
[45] Zhang S, Cao S, Zhang T, Yao Q, Lin H, Fisher A, et al. Overcoming the Technical Challenges in Al Anode-Based Electrochromic Energy Storage Windows. Small Methods 2020;4(1):1900545.
[46] Tong Z, Tian Y, Zhang H, Li X, Ji J, Qu H, et al. Recent advances in multifunctional electrochromic energy storage devices and photoelectrochromic devices. Sci China Chem 2017;60(1):13–37.
[47] Lu Z, Zhong X, Liu X, Wang J, Diao X. Energy storage electrochromic devices in the era of intelligent automation. Phys Chem Chem Phys 2021;23(26): 14126–45.

[48] Wang Z, Wang X, Cong S, Geng F, Zhao Z. Fusing electrochromic technology with other advanced technologies: A new roadmap for future development. Mater Sci Eng Rep 2020;140:100524.
[49] Kumar R, Pathak DK, Chaudhary A. Current status of some electrochromic materials and devices: a brief review. J Phys D: Appl Phys 2021;54:503002.
[50] Van Nguyen T, Do HH, Guo W, Tekalne M, Van Le Q, Nguyen TP, et al. Tungsten Oxide-Modified ITO Electrode for Electrochromic Window Based on Reversible Metal Electrodeposition. Electron Mater Lett 2021;18:36–46.
[51] Yao P, Xie S, Ye M, Yu R, Liu Q, Yan D, et al. Smart electrochromic supercapacitors based on highly stable transparent conductive graphene/CuS network electrodes. RSC Adv 2017;7(46):29088–95.
[52] Koo B-R, Jo M-H, Kim K-H, Ahn H-J. Amorphous-quantized WO3·H2O films as novel flexible electrode for advanced electrochromic energy storage devices. Chem Eng J 2021;424:130383.
[53] Yun TG, Kim D, Kim YH, Park M, Hyun S, Han SM. Photoresponsive Smart Coloration Electrochromic Supercapacitor. Adv Mater 2017;29(32):1606728.
[54] Zhang D, Sun B, Huang H, Gan Y, Xia Y, Liang C, et al. A Solar-Driven Flexible Electrochromic Supercapacitor. Mater 2020;13(5):1206.
[55] Shi Y, Sun M, Zhang Y, Cui J, Wang Y, Shu X, et al. Structure modulated amorphous/crystalline WO_3 nanoporous arrays with superior electrochromic energy storage performance. Solar Energ Mater Sol C 2020;212:110579.
[56] Li W, Zhang J, Zheng Y, Cui Y. High performance electrochromic energy storage devices based on Mo-doped crystalline/amorphous WO_3 core-shell structures. Solar Energ Mater S C 2022;235:111488.
[57] Wang M, He Y, Da Rocha M, Rougier A, Diao X. Temperature dependence of the electrochromic properties of complementary NiO//WO3 based devices. Solar Energ Mater S C 2021;230:111239.
[58] Hsiao Y-S, Chang-Jian C-W, Syu W-L, Yen S-C, Huang J-H, Weng H-C, et al. Enhanced electrochromic performance of carbon-coated V2O5 derived from a metal–organic framework. Appl Surf Sci 2021;542:148498.
[59] Ravi R, Surendren S, Deb B. Studies on All-Solid Electrochromic Devices Fabricated by a Bilayered Assembly of Hydrated Vanadium Pentoxide and PEDOT: PSS Coatings. Surf Inter 2021;22:100860.
[60] Zhao L, Kuang J, Zhuang W, Chao J, Liao W, Fu X, et al. Studies on transmittance modulation and ions transfer kinetic based on capacitive-controlled 2D V2O5 inverse opal film for electrochromic energy storage application. Nanotechnol 2021;33(5):054001.
[61] Xiong J, Yu L, Xia L, Fei A, Xu C, Chen S, et al. Fabrication of nitrogen doped TiO2-B nanotube film with novel electrochromic performance. Mater Sci Semiconductor Processing 2021:106347.
[62] Zhao L, Huang X, Lin G, Peng Y, Chao J, Yi L, et al. Structure engineering in hexagonal tungsten trioxide/oriented titanium dioxide nanorods arrays with high performances for multi-color electrochromic energy storage device applications. Chem Eng J 2021;420:129871.
[63] Zhang B, Tian Y, Chi F, Liu S. Synthesis of nitrogen-doped carbon embedded TiO_2 films for electrochromic energy storage application. Electrochim Acta 2021;390:138821.
[64] Chavan HS, Hou B, Jo Y, Inamdar AI, Im H, Kim H. Optimal Rule-of-Thumb Design of Nickel-Vanadium Oxides as an Electrochromic Electrode with Ultrahigh Capacity and Ultrafast Color Tunability. ACS Appl Mater Inter 2021;13:57403–10.
[65] Kim K-H, Jeong S-J, Koo B-R, Ahn H-J. Surface amending effect of N-doped carbon-embedded NiO films for multirole electrochromic energy-storage devices. Appl Surf Sci 2021;537:147902.
[66] Bakar SA, Ahmed S, Ehsan MA, Ahmed H, Baig R, Abbas SM, et al. Interlinked polyaniline nanostructure for enhanced electrochromic performance. Mater Chem Phy 2021:125391.
[67] Lin T, Liu W, Yan B, Li J, Lin Y, Zhao Y, et al. Self-Assembled Polyaniline/Ti3C2Tx Nanocomposites for High-Performance Electrochromic Films. Nanomater 2021;11(11):2956.
[68] Lv H, Yang S, Li C, Han C, Tang Y, Li X, et al. Suppressing passivation layer of Al anode in aqueous electrolytes by complexation of H2PO4− to Al3+ and an electrochromic Al ion battery. Energy Storage Mater 2021;39:412–8.
[69] Li W, Sun J, Zhang J, Ganiyat OA, Cui Y. Facile fabrication of W18O49/PEDOT: PSS/ITO-PET flexible electrochromic films by atomizing spray deposition. Res Surf Inter 2021;2:100002.
[70] Do M, Park C, Bae S, Kim J, Kim JH. Design of highly stable and solution-processable electrochromic devices based on PEDOT: PSS. Org Electron 2021;93:106106.
[71] Zhou K, Wang H, Jiu J, Liu J, Yan H, Suganuma K. Polyaniline films with modified nanostructure for bifunctional flexible multicolor electrochromic and supercapacitor applications. Chem Eng J 2018;345:290–9.
[72] Li Y, Yan L, Zhang L, Song X, Dai C. Design of electrochromic supercapacitor based on rGO–W18O49 nanowires/polyaniline. J Mater Sci Mater Electron 2021;32(14):19179–90.
[73] Liu L, Wang T, He Z, Yi Y, Wang M, Luo Z, et al. All-solid-state electrochromic Li-ion hybrid supercapacitors for intelligent and wide-temperature energy storage. Chem Eng J 2021;414:128892.
[74] Wei D, Scherer MR, Bower C, Andrew P, Ryhänen T, Steiner U. A nanostructured electrochromic supercapacitor. Nano lett 2012;12(4):1857–62.
[75] Shen L, Du L, Tan S, Zang Z, Zhao C, Mai W. Flexible electrochromic supercapacitor hybrid electrodes based on tungsten oxide films and silver nanowires. Chem Commun 2016;52(37):6296–9.
[76] Lv X, Li J, Zhang L, Ouyang M, Tameev A, Nekrasov A, et al. High-performance electrochromic supercapacitor based on quinacridone dye with good specific capacitance, fast switching time and robust stability. Chem Eng J 2021;133733.
[77] Ojha M, Pal M, Deepa M. Variable-Tint Electrochromic Supercapacitor with a Benzyl Hexenyl Viologen-Prussian Blue Architecture and Ultralong Cycling Life. ACS Appl Electron Mater 2023;5:2401–13.
[78] Xue J, Li W, Song Y, Li Y, Zhao J. Visualization electrochromic-supercapacitor device based on porous Co doped NiO films. J Alloy Comp 2021;857:158087.
[79] Sun B, Liu Z, Li W, Huang H, Xia Y, Gan Y, et al. A high-performance electrochromic battery based on complementary Prussian white/Li4Ti5O12 thin film electrodes. Solar Energ Mater Sol C 2021;231:111314.
[80] Poh WC, Gong X, Yu F, Lee PS. Electropolymerized 1D Growth Coordination Polymer for Hybrid Electrochromic Aqueous Zinc Battery. Adv Sci 2021;8(21):2101944.
[81] Tang X, Chen J, Wang Z, Hu Z, Song G, Zhang S, et al. Vibrant Color Palettes of Electrochromic Manganese Oxide Electrodes for Colorful Zn-Ion Battery. Adv Opt Mater 2021;9(19):2100637.
[82] Zhang W, Li H, Yu WW, Elezzabi AY. Emerging Zn Anode-Based Electrochromic Devices. Small Sci 2021:2100040.
[83] Xie J, Yang P, Wang Y, Qi T, Lei Y, Li CM. Puzzles and confusions in supercapacitor and battery: Theory and solutions. J Power Sources 2018;401:213–23.
[84] Xiang X, Zhang W, Yang Z, Zhang Y, Zhang H, Zhang H, et al. Smart and flexible supercapacitor based on a porous carbon nanotube film and polyaniline hydrogel. RSC adv 2016;6(30):24946–51.
[85] Wang J, Liu J, Hu M, Zeng J, Mu Y, Guo Y, et al. A flexible, electrochromic, rechargeable Zn//PPy battery with a short circuit chromatic warning function. J Mater Chem A 2018;6(24):11113–8.
[86] Sun S, Tang C, Jiang Y, Wang D, Chang X, Lei Y, et al. Flexible and rechargeable electrochromic aluminium-ion battery based on tungsten oxide film electrode. Solar Energ Mater Sol C 2020;207:110332.
[87] Hao T, Wang S, Xu H, Zhang X, Xue J, Liu S, et al. Stretchable electrochromic devices based on embedded WO3@AgNW Core-Shell nanowire elastic conductors. Chem Eng J 2021;426:130840.
[88] Zhai Y, Li Y, Zhang H, Yu D, Zhu Z, Sun J, et al. Self-rechargeable-battery-driven device for simultaneous electrochromic windows, ROS biosensing, and energy storage. ACS Appl Mater Interfaces 2019;11(31):28072–7.
[89] L. Manjakkal, S. Dervin, R. Dahiya, Flexible potentiometric pH sensors for wearable systems, RSC Adv. 10(15) (2020) 8594-8617. (Self-reference).
[90] Che B, Zhou D, Li H, He C, Liu E, Lu X. A highly bendable transparent electrode for organic electrochromic devices. Org Electron 2019;66:86–93.
[91] Shakhnov VA, Vlasov AI, Tokarev SV. Electrochromic thin-film components for information representation systems. IOP Conference Series: Materials Science and Engineering 2016;151:012005.

[92] Wang M, Diao X, Dong G, He Y, Liu Q. Optical, electrical, and electrochemical properties of indium tin oxide thin films studied in different layer-structures and their corresponding inorganic all-thin-film solid-state electrochromic devices. J Vac Sci TechnolA 2017;35(2):021512.
[93] Macher S, Rumpel M, Schott M, Posset U, Giffin GA, Löbmann P. Avoiding Voltage-Induced Degradation in PET-ITO-Based Flexible Electrochromic Devices. ACS Appl Mater Inter 2020;12(32):36695–705.
[94] Hong K, Cho M, Kim SO. Atomic Layer Deposition Encapsulated Activated Carbon Electrodes for High Voltage Stable Supercapacitors. ACS Appl Mater Inter 2015;7(3):1899–906.
[95] Guan C, Liu J, Wang Y, Mao L, Fan Z, Shen Z, et al. Iron oxide-decorated carbon for supercapacitor anodes with ultrahigh energy density and outstanding cycling stability. ACS Nano 2015;9(5):5198–207.
[96] Zhang G, Hu J, Nie Y, Zhao Y, Wang L, Li Y, et al. Integrating Flexible Ultralight 3D Ni Micromesh Current Collector with NiCo Bimetallic Hydroxide for Smart Hybrid Supercapacitors. Adv Funct Mater 2021;31(24):2100290.
[97] Hu W, Niu X, Li L, Yun S, Yu Z, Pei Q. Intrinsically stretchable transparent electrodes based on silver-nanowire–crosslinked-polyacrylate composites. Nanotechnol 2012;23(34):344002.
[98] Liu H-S, Pan B-C, Liou G-S. Highly transparent AgNW/PDMS stretchable electrodes for elastomeric electrochromic devices. Nanoscale 2017;9(7):2633–9.
[99] Li H, Xie K, Pan Y, Yao M, Xin C. Variable emissivity infrared electrochromic device based on polyaniline conducting polymer. Synthetic Met 2009;159(13):1386–8.
[100] Wang H, Barrett M, Duane B, Gu J, Zenhausern F. Materials and processing of polymer-based electrochromic devices. Mater Sci Eng B 2018;228:167–74.
[101] Alves RD, Rodrigues LC, Andrade JR, Fernandes M, Pinto JV, Pereira L, et al. GelatinnZn(CF3SO3)2 Polymer Electrolytes for Electrochromic Devices. Electroanal 2013;25(6):1483–90. self-reference.
[102] Agnihotry SA, Nidhi P, Sekhon SS. Li+ conducting gel electrolyte for electrochromic windows. Solid State Ion 2000;136–137:573–6.
[103] Granqvist CG. Oxide electrochromics: An introduction to devices and materials. Solar Energ Mater Sol C 2012;99:1–13.
[104] Xu W-W, Zhao S-Q, Chen C, Liu Y-H. Flexible electrochromic supercapacitor based on multifunctional hydrogel. In: IOP Conference Series: Earth and Environmental Science. IOP Publishing; 2021. p. 012214.
[105] Lu Z, Zhong X, Liu X, Wang J, Diao X. Energy storage electrochromic devices in the era of intelligent automation. Phys Chem Chem Phys 2021;23:14126–45.
[106] Nawaz M, Sliman Y, Ercan I, Lima-Tenório MK, Tenório-Neto ET, Kaewsaneha C, et al. 2 - Magnetic and pH-responsive magnetic nanocarriers. In: Makhlouf ASH, Abu-Thabit NY, editors. Stimuli Responsive Polymeric Nanocarriers for Drug Delivery Applications. Woodhead Publishing; 2019. p. 37–85.
[107] Ma D, Niu H, Huang J, Li Q, Sun J, Cai H, et al. Porous NiMoO4 Nanosheet Films and a Device with Ultralarge Optical Modulation for Electrochromic Energy-Storage Applications. Nano Lett 2024.
[108] Zhao J, Zhang S, Chang S, Li C, Fang C, Xia X, et al. A flexible electrochromic device with variable infrared emissivity based on $W_{18}O_{49}$ nanowire cathode and MXene infrared transparent conducting electrode. Chem Eng J 2024;480:148010.
[109] Manjakkal L, Sakthivel B, Gopalakrishnan N, Dahiya R. Printed flexible electrochemical pH sensors based on CuO nanorods. Sens Actuat B: Chem 2018;263:50–8. self-reference.
[110] Bi Z, Li X, Chen Y, Xu X, Zhang S, Zhu Q. Bi-functional flexible electrodes based on tungsten trioxide/zinc oxide nanocomposites for electrochromic and energy storage applications. Electrochim Acta 2017;227:61–8.
[111] Shaikh SF, Ubaidullah M, Mane RS, Al-Enizi AM. Chapter 4 - Types, Synthesis methods and applications of ferrites. In: Mane RS, Jadhav VV, editors. Spinel Ferrite Nanostructures for Energy Storage Devices. Elsevier; 2020. p. 51–82.
[112] Sahu B, Bansal L, Rath DK, Kandpal S, Ghosh T, Ahlawat N, et al. Bendable & twistable oxide-polymer based hybrid electrochromic device: Flexible and multi-wavelength color modulation. Mater Today Electron 2024;7:100082.
[113] Nayak L, Mohanty S, Nayak SK, Ramadoss A. A review on inkjet printing of nanoparticle inks for flexible electronics. J Mater Chem C 2019;7(29):8771–95.
[114] Wu W, Fang H, Ma H, Wu L, Wang Q, Wang H. Self-Powered Rewritable Electrochromic Display based on WO_{3-x} Film with Mechanochemically Synthesized MoO_{3-y} Nanosheets. ACS Appl Mater Inter 2021;13(17):20326–35.
[115] Costa C, Pinheiro C, Henriques I, Laia CAT. Inkjet Printing of Sol-Gel Synthesized Hydrated Tungsten Oxide Nanoparticles for Flexible Electrochromic Devices. ACS Appl Mater Inter 2012;4(3):1330–40.
[116] Costa C, Pinheiro C, Henriques I, Laia CAT. Electrochromic Properties of Inkjet Printed Vanadium Oxide Gel on Flexible Polyethylene Terephthalate/Indium Tin Oxide Electrodes. ACS Appl Mater Inter 2012;4(10):5266–75.
[117] A. Bashir, T.I. Awan, A. Tehseen, M.B. Tahir, M. Ijaz, Chapter 3 - Interfaces and surfaces, in: T.I. Awan, A. Bashir, A. Tehseen (Eds.), Chemistry of Nanomaterials, Elsevier2020, pp. 51-87.
[118] Cai G, Zhu R, Liu S, Wang J, Wei C, Griffith KJ, et al. Tunable Intracrystal Cavity in Tungsten Bronze-Like Bimetallic Oxides for Electrochromic Energy Storage. Adv Energ Mater 2021:2103106.
[119] Chen Y, Wang Y, Sun P, Yang P, Du L, Mai W. Nickel oxide nanoflake-based bifunctional glass electrodes with superior cyclic stability for energy storage and electrochromic applications. J Mater Chem A 2015;3(41):20614–8.
[120] Kharade RR, Mali SS, Patil SP, Patil KR, Gang MG, Patil PS, et al. Enhanced electrochromic coloration in Ag nanoparticle decorated WO_3 thin films. Electrochim Acta 2013;102:358–68.
[121] Jo M-H, Koo B-R, Ahn H-J. Defective impacts on amorphous $WO_3{\cdot}H_2O$ films using accelerated hydrolysis effects for flexible electrochromic energy-storage devices. Appl Surf Sci 2021;556:149664.
[122] Aljafari B, Indrakar SK, Ram MK, Biswas PK, Stefanakos E, Takshi A. A Polyaniline-Based Redox-Active Composite Gel Electrolyte with Photo-Electric and Electrochromic Properties. ChemElectroChem 2019;6(23):5888–95.
[123] Wang K, Wu H, Meng Y, Zhang Y, Wei Z. Integrated energy storage and electrochromic function in one flexible device: an energy storage smart window. Energ Environ Sci 2012;5(8):8384–9.
[124] Guo Y, Li W, Yu H, Perepichka DF, Meng H. Flexible Asymmetric Supercapacitors via Spray Coating of a New Electrochromic Donor-Acceptor Polymer. Adv Energ Mater 2017;7(2):1601623.
[125] Zhao X, Li Z, Guo Q, Yang X, Nie G. High performance organic-inorganic hybrid material with multi-color change and high energy storage capacity for intelligent supercapacitor application. J Alloy Comp 2021;855:157480.
[126] Tian Y, Cong S, Su W, Chen H, Li Q, Geng F, et al. Synergy of W18O49 and Polyaniline for Smart Supercapacitor Electrode Integrated with Energy Level Indicating Functionality. Nano Lett 2014;14(4):2150–6.
[127] Guo Q, Li J, Zhang B, Nie G, Wang D. High-Performance Asymmetric Electrochromic-Supercapacitor Device Based on Poly(indole-6-carboxylicacid)/TiO2 Nanocomposites. ACS Appl Mater Inter 2019;11(6):6491–501.
[128] Zhang H, Tian Y, Wang S, Feng J, Hang C, Wang C, et al. Robust Cu-Au alloy nanowires flexible transparent electrode for asymmetric electrochromic energy storage device. Chem Eng J 2021;426:131438.
[129] Jiao X, Li G, Yuan Z, Zhang C. High-Performance Flexible Electrochromic Supercapacitor with a Capability of Quantitative Visualization of Its Energy Storage Status through Electrochromic Contrast. ACS Appl Energ Mater 2021;4(12):14155–68.
[130] Wang Y, Jiang H, Zheng R, Pan J, Niu J, Zou X, et al. A flexible, electrochromic, rechargeable Zn-ion battery based on actiniae-like self-doped polyaniline cathode. J Mater Chem A 2020;8:12799–809.
[131] Ding Y, Wang M, Mei Z, Diao X. Flexible Inorganic All-Solid-State Electrochromic Devices toward Visual Energy Storage and Two-Dimensional Color Tunability. ACS Appl Mater Inter 2023;15(12):15646–56.
[132] Macher S, Schott M, Dontigny M, Guerfi A, Zaghib K, Posset U, et al. Large-Area Electrochromic Devices on Flexible Polymer Substrates with High Optical Contrast and Enhanced Cycling Stability. Adv Mater Technol 2021;6(2):2000836.
[133] Wang L, Zhang X, Chen X, Li X, Zhao Y, Li W, et al. A large-area, flexible, high contrast and long-life stable solid-state electrochromic device driven by an anion-assisted method. J Mater Chem C 2021;9(5):1641–8.
[134] Abbel R, Galagan Y, Groen P. Roll-to-Roll Fabrication of Solution Processed Electronics. Adv Eng Mater 2018;20:1701190.

[135] Palavesam N, Marin S, Hemmetzberger D, Landesberger C, Bock K, Kutter C. Roll-to-roll processing of film substrates for hybrid integrated flexible electronics. Flexible Printed Electron 2018;3(1):014002.
[136] Lin S, Bai X, Wang H, Wang H, Song J, Huang K, et al. Roll-to-Roll Production of Transparent Silver-Nanofiber-Network Electrodes for Flexible Electrochromic Smart Windows. Adv Mater 2017;29(41):1703238.
[137] Simon P, Gogotsi Y. The path to high-rate energy storage goes through narrow channels. Joule 2022;6(1):28–30.
[138] Baig MM, Gul IH, Baig SM, Shahzad F. 2D MXenes: Synthesis, properties, and electrochemical energy storage for supercapacitors–A review. J Electroanal Chem 2022;904:115920.
[139] Gao X, Du X, Mathis TS, Zhang M, Wang X, Shui J, et al. Maximizing ion accessibility in MXene-knotted carbon nanotube composite electrodes for high-rate electrochemical energy storage. Nature commun 2020;11(1):1–9.
[140] Xi W, Jin J, Zhang Y, Wang R, Gong Y, He B, et al. Hierarchical MXene/transition metal oxide heterostructures for rechargeable batteries, capacitors, and capacitive deionization. Nanoscale 2022;14(33):11923–44.
[141] Liu Y-T, Zhang P, Sun N, Anasori B, Zhu Q-Z, Liu H, et al. Self-Assembly of Transition Metal Oxide Nanostructures on MXene Nanosheets for Fast and Stable Lithium Storage. Adv Mater 2018;30(23):1707334.
[142] Li R, Ma X, Li J, Cao J, Gao H, Li T, et al. Flexible and high-performance electrochromic devices enabled by self-assembled 2D TiO2/MXene heterostructures. Nature Commun 2021;12(1):1587.
[143] Tang C-J, Ye J-M, Yang Y-T, He J-L. Large-area flexible monolithic ITO/WO3/Nb2O5/NiVOχ/ITO electrochromic devices prepared by using magnetron sputter deposition. Opt Mater 2016;55:83–9.
[144] Lee E, Yazdanian M, Selkowitz S. The energy-savings potential of electrochromic windows in the UScommercial buildings sector. Berkeley, CA (US): Ernest Orlando Lawrence Berkeley NationalLaboratory; 2004.
[145] Cannavale A, Ayr U, Fiorito F, Martellotta F. Smart electrochromic windows to enhance building energy efficiency and visual comfort. Energies 2020;13(6):1449.
[146] Bui D-K, Nguyen TN, Ghazlan A, Ngo TD. Biomimetic adaptive electrochromic windows for enhancing building energy efficiency. Appl Energ 2021;300:117341.
[147] Kim J-H, Hong J, Han S-H. Optimized Physical Properties of Electrochromic Smart Windows to Reduce Cooling and Heating Loads of Office Buildings. Sustainability 2021;13(4):1815.
[148] Yang S-H, Yang J-H, Chen Z-Y, Ho C-C. High optical contrast and radiant heat blocking properties of hierarchically structured electrodes for electrochromic windows. J Alloy Comp 2021;160762.
[149] Kou Z, Wang J, Tong X, Lei P, Gao Y, Zhang S, et al. Multi-functional electrochromic energy storage smart window powered by CZTSSe solar cell for intelligent managing solar radiation of building. Solar Energ Mater Sol C 2023;254:112273.
[150] Pérez-Lombard L, Ortiz J, Pout C. A review on buildings energy consumption information. Energ Buildings 2008;40(3):394–8.
[151] Cao X, Dai X, Liu J. Building energy-consumption status worldwide and the state-of-the-art technologies for zero-energy buildings during the past decade. Energ Buildings 2016;128:198–213.
[152] Cai G, Park S, Cheng X, Eh A-L-S, Lee PS. Inkjet-printed metal oxide nanoparticles on elastomer for strain-adaptive transmissive electrochromic energy storage systems. Sci Technol Adv Mater 2018;19(1):759–70.
[153] He Z, Gao B, Li T, Liao J, Liu B, Liu X, et al. Piezoelectric-driven self-powered patterned electrochromic supercapacitor for human motion energy harvesting. ACS Sust Chem Eng 2018;7(1):1745–52.
[154] L. Manjakkal, L. Yin, A. Nathan, J. Wang, R. Dahiya, Energy Autonomous Sweat-Based Wearable Systems, Adv. Mater. 33(35) (2021) 2100899. (self-reference).
[155] Seneviratne S, Hu Y, Nguyen T, Lan G, Khalifa S, Thilakarathna K, et al. A Survey of Wearable Devices and Challenges. IEEE Commun Surv Tut 2017;19(4):2573–620.
[156] Xu C, Song Y, Han M, Zhang H. Portable and wearable self-powered systems based on emerging energy harvesting technology. Microsys Nanoeng 2021;7(1):25.
[157] Ates HC, Nguyen PQ, Gonzalez-Macia L, Morales-Narváez E, Güder F, Collins JJ, et al. End-to-end design of wearable sensors. Nature Rev Mater 2022;7(11):887–907.
[158] Hartel MC, Lee D, Weiss PS, Wang J, Kim J. Resettable sweat-powered wearable electrochromic biosensor. Biosens Bioelectron 2022;215:114565.
[159] Lv J, Yin L, Chen X, Jeerapan I, Silva CA, Li Y, et al. Wearable Biosupercapacitor: Harvesting and Storing Energy from Sweat. Adv Funct Mater 2021;31(38):2102915.
[160] Li J, Yang P, Li X, Jiang C, Yun J, Yan W, et al. Ultrathin Smart Energy-Storage Devices for Skin-Interfaced Wearable Electronics. ACS Energ Lett 2023;8(1):1–8.
[161] Singh SB, Tran DT, Jeong K-U, Kim NH, Lee JH. A Flexible and Transparent Zinc-Nanofiber Network Electrode for Wearable Electrochromic, Rechargeable Zn-Ion Battery. Small 2022;18(5):2104462.
[162] Nejat P, Jomehzadeh F, Taheri MM, Gohari M, Abd MZ. Majid, A global review of energy consumption, CO2 emissions and policy in the residential sector (with an overview of the top ten CO2 emitting countries). Renew Sust Energ Rev 2015;43:843–62.
[163] K.G. Logan, J.D. Nelson, A. Hastings, Low emission vehicle integration: Will National Grid electricity generation mix meet UK net zero?, Proceedings of the Institution of Mechanical Engineers, Part A: J. Power Energy (2021) 09576509211015472.
[164] Schott M, Niklaus L, Müller C, Bozkaya B, Giffin GA. Flexible electrochromic devices prepared on ultra-thin ITO glass. Mater Adv 2021;2(14):4659–66.
[165] Cao X, Lau C, Liu Y, Wu F, Gui H, Liu Q, et al. Fully Screen-Printed, Large-Area, and Flexible Active-Matrix Electrochromic Displays Using Carbon Nanotube Thin-Film Transistors. ACS Nano 2016;10(11):9816–22.
[166] E. Kumi Barimah, E., D. E. Anagnostou, G. Jose, Phase changeable vanadium dioxide (VO_2) thin films grown from vanadium pentoxide (V_2O_5) using femtosecond pulsed laser deposition. AIP Advances,10 (2020) 065225. (self-reference).
[167] E. Kumi Barimah, S. Rahayu, M. W. Ziarko, N. Bamiedakis, I. H. White, R. V. Penty, R. V.G. M. Kale, G. Jose, Erbium-Doped Nanoparticle–Polymer Composite Thin Films for Photonic Applications: Structural and Optical Properties. ACS Omega, 5(2020), 9224-9232. (self-reference).
[168] E. Kumi Barimah, M. W. Ziarko, N. Bamiedakis, I. H. White, R. V. Penty, R. V., G. Jose, Erbium-doped glass nanoparticle embedded polymer thin films using femtosecond pulsed laser deposition. Optical Materials Express, 8 (2018), 1997-2007. (self-reference).
[169] H. Guo, T. Shi, F. Wang, L. Zhang, Z. Lin, Adaptive clustering-based hierarchical layout optimization for large-scale integrated energy systems, IET Renew. Power Genera., 14(2021), 3336-3345, (self-reference).
[170] Z. Qian, J. Wu, X. He, Z. Lin, Power maximised and anti-saturation power conditioning circuit for current transformer harvester on overhead lines, IET Power Electronics, 11(2018), 2271-2278. (self-reference).

Dr. Libu Manjakkal (PhD, MRSC): Libu Manjakkal received BSc (2006)., MSc (2008). degrees in physics from Calicut University and Mahatma Gandhi University, India. From 2009 to 2012, he was with CMET, Thrissur, India and in 2012 for short period he worked at NOVA School of Science and Technology Lisbon, Portugal. He completed Ph.D. in electronic engineering from the Institute of Electron Technology, Poland (2012–2015) (Marie Curie ITN Program). Between 2016-2022, he has been a post-doctoral fellow in University of Glasgow in various roles. Currently he is lecturer at Edinburgh Napier University with research focus on material synthesis, wearable energy storage, electrochemical sensors, supercapacitors, electrochromic energy storage and energy autonomous sensing systems. He has authored/co-authored more than 75 peer-review papers (50 journals) with 3700+ citation and h index 30. He was shortlisted for important awards such as by the European Commission for Marie Curie Awards in the "Promising Research Talent" category, "Outstanding Young Scientists Scholarship Award" from the Polish Ministry of higher education and RIENG 2024 Young Investigator Award. He is currently editor of Results in Engineering Journal, ELSEVIER.

Asso. Prof. Luis Pereira: Luis Pereira is Associate Professor at the School of Science and Technology - NOVA University Lisbon and currently CTO of the AlmaScience Colab. He has coordinated and participated in several R&D projects under different funding schemes, including industry direct funding ones. He has been granted in 2015 with a Starting Grant of the European Research Council (ERC) on the development of cellulose nanocomposites for paper electronics (New-Fun, project 640598). Recent research interests were on the design and synthesis of 1D, 2D and 3D inorganic and hybrid nanostructures, chiral cellulose nanocomposites, functional micro and nanofibers and its integration on chromogenic, electronic and electrochemical devices. Luis Pereira has published more than 180 papers and has a h-index of 53 with close to 13000 citations (Google Scholar). He was involved in the first demonstration of oxide transistors using paper ad dielectric and substrate. This resulted in a family of 14 patents.

Dr Eric Kumi Barimah received a B.Sc. degree in physics from the Kwame Nkrumah University of Science and Technology, Kumasi, Ghana, in 2001, an M.S. degree in electrical engineering from Colourado Technical University, Colourado Springs, CO, USA, in 2007, and the PhD degree from Hampton University, Hampton, VA, USA, in 2014. In 2015, he joined the School of Chemical and Process Engineering, University of Leeds, Leeds, U.K., as an Experimental Officer in the Ultrafast Laser Plasma Implantation facility. He is currently a Senior Research Fellow in Bioceramic Materials at the University of Leeds. He has over 7 years of experience in photonic integration with ultrafast laser plasma-assisted doping process, phase-changed material and metal oxide thin films, polymer nanocomposite thin films and characterisations. Prior to Leeds, he held a post-doctoral position at Hampton University in the USA, where he specialised in laser interactions with matter, laser-induced breakdown spectroscopy (LIBS) in the infrared, laser spectroscopy, and ceramic crystal glass growth in the USA. He has over 35 peer review research publications. Selected publications:

Dr. Paul Grey received his master's degree in micro- and nanotechnology in 2014 with a work on the "Development of WO3 Electrochromic Thin-Film Transistors on Flexible Substrates". He then worked as a researcher on the project A3Ple with the fabrication of printed electrochromic displays on paper substrates for applications such as packaging. In 2021 Paul finished his PhD in the field of chiral nematic films of cellulose nanocrystals (CNCs) and its application in photonics and optoelectronic devices. His scientific interests evolve around Electrolyte Gated Transistors, Cellulose-based nanocomposites, Oxide nanoparticles (WO3, ZnO), Electrochromic materials, Printing technologies, and Photonic films from Chiral CNCs.

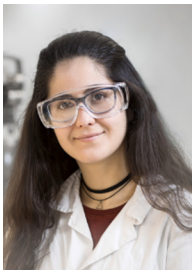

Fabiane F. Franco graduated in Physical and Biomolecular Sciences at the University of São Paulo, Brazil and received her master's degree in Nanoscience from Aarhus University, Denmark in 2018 where she submitted her thesis on metal organic frameworks for CO2 storage and catalysis. Fabiane is currently a Marie Curie Early Stage Researcher and PhD student at the Water and Environment group at the University of Glasgow, Scotland. She specializes in materials science and characterization techniques, focusing on the development of electrochemical sensors using different printing technologies and nanomaterials for real-time monitoring.

Dr Zhengyu Lin is a Reader with the Centre for Renewable Energy Systems Technology (CREST), Loughborough University, U.K.. His research interests include power electronics and its applications in renewable energy, energy storage, microgrids, and multi-energy systems. . ZL has 20+ years research experience in power electronics and microgrids based energy systems, and has published over 70 peer-reviewed papers (1500+ citations and h-Index of 20).

Prof. Gin Jose: Chair in Functional Materials, an expert in photonic materials and sensor devices. GJ has excellent track record in translating original research into applications through commercialization with 4 patents (WO/2011/030157, WO/2013/132252, WO2013117941A2, and WO2017025759A1) and two spinouts on advanced materials for photonics and biosensors. GJ is currently the PI of EPSRC £1.7M (EP/T004711/1) project on photonic biosensing and imaging and a recently concluded £2.5M multi-university/industry project on photonic integration (Seamatics, EP/M015165/1), which is linked to the £1.2M strategic equipment for manufacturing (EP/M015165/1) which will form the basis for materials engineering in ELCTROSEND. GJ's group have been successful in Medipex NHS innovation, Royal Society of Chemistry Emerging Technology and Royal Academy of Engineering ERA Entrepreneurship awards. GJ was Co-I of two BBSRC projects, PI of NIHR i4i and EU H2020 project on biosensors, other Industry funded projects, Co-I in two innovate UK projects with total value of ~£1M. GJ has >150 research publications (3000+citations, H-index 28) and is currently the main supervisor of four PhD students and 5 postdocs.

Prof. Richard A Hogg (RH) was awarded a Ph.D. in Physics in 1995 from The University of Sheffield, and then spent two years as a post-doctoral researcher at NTT Basic Research Laboratories in Atsugi, Japan. RH was then awarded an EU-Japan fellowship as a visiting researcher in Professor Arakawa's Laboratory at the University of Tokyo, Japan. RH subsequently spent three years at Toshiba Research Europe's Cambridge Laboratory, before moving to a Agilent Technologies Fibre-Optic Component Operation in Ipswich, U.K., in 2000. At the time this was the largest III-V facility in Europe. In 2003 RH joined the Electronic and Electrical Engineering Department, The University of Sheffield, resuming an academic career focused on developing the understanding of device physics and engineering, epitaxial processes, fabrication technologies and applications of various semiconductor devices such as lasers, amplifiers, superluminescent light emitting diode devices, and resonant tunneling diodes. RH moved to The University of Glasgow in August 2015, served as Director of Research for The School of Engineering from August 2016 to July 2018, and was appointed head of the Electronics and Nano-Engineering Division in August 2018. In 2020 he spun out two companies, III-V Epi Ltd (epitaxial wafer foundry), and Vector Photonics Ltd (PCSELs). RH moved to Aston University in May 2023.